

# Thermodynamic Properties of Organic Substances: Experiment, Modeling, and Technological Applications

Gennady J. Kabo<sup>a</sup>, Andrey V. Blokhin<sup>a</sup>, Eugene Paulechka<sup>b\*</sup>, Gennady N. Roganov<sup>c</sup>, Michael Frenkel<sup>b,\*\*</sup>, Iosif A. Yursha<sup>d†</sup>, Vladimir Diky<sup>b</sup>, Dzmitry Zaitsau<sup>e</sup>, Ala Bazyleva<sup>b</sup>, Vladimir V. Simirsky<sup>f</sup>, Larisa S. Karpushenkava<sup>a</sup>, Viktor M. Sevruk<sup>a</sup>

<sup>a</sup>Chemistry Department, Belarusian State University, 14 Leningradskaya Street, 220030 Minsk, Belarus

<sup>b</sup>Thermodynamics Research Center, Applied Chemicals and Materials Division, National Institute of Standards and Technology, 325 Broadway, Boulder, Colorado 80305-3337, USA

<sup>c</sup>Department of Chemical Engineering, Mogilev State University of Food Technologies, 3 Shmidt Prospekt, 212027 Mogilev, Belarus

<sup>d</sup>JSC Grodno Azot, 100 Prospekt Kosmonavtov, 230013 Grodno, Belarus

<sup>e</sup>Department of Physical Chemistry, University of Rostock, Dr.-Lorenz-Weg 2, D-18059 Rostock, Germany

<sup>f</sup>Pilot Production, Institute of Bioorganic Chemistry, National Academy of Sciences, 5/3 Academician V. F. Kuprevich Street, 220144 Minsk, Belarus

---

\*Corresponding author, e-mail address: [yauheni.paulechka@nist.gov](mailto:yauheni.paulechka@nist.gov)

\*\*Retired. Current address: 4055 Victory Drive, Frisco TX 75034, USA

†Deceased

## **Abstract**

In this review, results of the studies of thermodynamic properties of organic substances conducted at the Chemistry Department of the Belarusian State University (Minsk, Belarus) over a period of more than 50 years are summarized. Emphasis is made on precise measurements (both calorimetry and equilibria) and prediction methods, including group-contribution, quantum chemical, and statistical mechanical, for a broad range of thermodynamic properties of various classes of chemical substances. The principal purposes of these studies were to establish relationships between thermodynamic properties of organic substances and their molecular structure, develop methods of extrapolation and prediction of the properties of substances lacking experimental data, and provide thermodynamic background for innovative energy- and resource-saving technologies.

## **1. Introduction**

Over a period of more than 50 years, a large number of studies of thermodynamic properties of organic substances were conducted at the Chemistry Department of the Belarusian State University (Minsk, Belarus). Our cross-generational team, united by enthusiasm for the subject matter and mutual trust, gained strength from the breadth of interests and technical skills present in its members. Our research was inspired by the scientific traditions established by Frederick D. Rossini [1], Kenneth S. Pitzer [2], Edgar F. Westrum, Jr. and John P. McCullough [3], Sergey M. Skuratov and Viktor P. Kolesov [4], and Vladimir M. Tatevsky [5]. Our studies were designed to generate high-precision experimental measurements of the thermodynamic properties of organic compounds, elucidate relationships between thermodynamic properties of organic substances and their molecular structure, create methods of extrapolation and prediction of the properties of substances lacking experimental data, and provide a thermodynamic background for innovative energy- and resource-saving technologies.

## **2. Experimental methods**

Original apparatuses for high-precision experimental measurements of a wide variety of fundamental thermodynamic parameters were designed, built, or improved [6], including for: enthalpies of chemical reactions; enthalpies of phase transitions such as crystal-to-crystal, crystal-to-liquid, crystal-to-gas, and liquid-to-gas; and heat capacities of and vapor pressure over various phases. These parameters are of critical importance for thermodynamic characterization of individual substances and chemical reactions and for relating molecular structures and properties, as expressed in correlations and group contributions. These are also valuable data for innovative

industrial developments such as energy-saving chemical engineering technologies, methods of fuel production from plant biomass, and processes in gas-generating and thermostabilizing systems.

### 2.1. Chemical equilibria

One of the most important problems in chemical thermodynamics is determining equilibrium compositions in chemical reactions based on their standard enthalpies  $\Delta_r H_T^\circ$  and entropies  $\Delta_r S_T^\circ$ . Our research has clearly demonstrated that solving the reverse problem is a powerful method for obtaining these quantities. Based on temperature dependences of equilibrium constants  $K$ , we use the equations:

$$\begin{aligned} RT^2 \left( \frac{\partial \ln K}{\partial T} \right)_p &= \Delta_r H_T^\circ, \\ R \left( \frac{\partial (T \ln K)}{\partial T} \right)_p &= \Delta_r S_T^\circ. \end{aligned} \quad (1)$$

Experimental studies of chemical equilibria to determine the thermodynamic parameters of the reactions were initiated by Prof. D. N. Andreevsky. At the beginning of these efforts, the most significant drawback was the absence of a universal experimental technique for achieving and quantifying equilibria of reactions involving various classes of chemical compounds.

To address this challenge, we developed various experimental techniques applying appropriate external conditions, using efficient catalysts to assure desired selectivity and rates of the reactions, and choosing temperature ranges suitable for high-precision determination of the reaction enthalpies and entropies. Essential to these experiments, is confidence that chemical equilibrium has been achieved, and so experimental design included various compositions of initial reactants or their solutions as well as varying initial contact time between the reactants or their contact time with a catalyst [7, 8].

We have shown that the best precision in determination of reaction enthalpies and entropies can be achieved by using gas-liquid chromatography for analysis of equilibrium compositions. The equilibria were studied with experimental apparatuses of three types: a static thermostated reactor with periodic sample analysis, a dynamic flow reactor equipped with a dosing pump (figure 1), and a pulse chromatographic apparatus (figure 2).

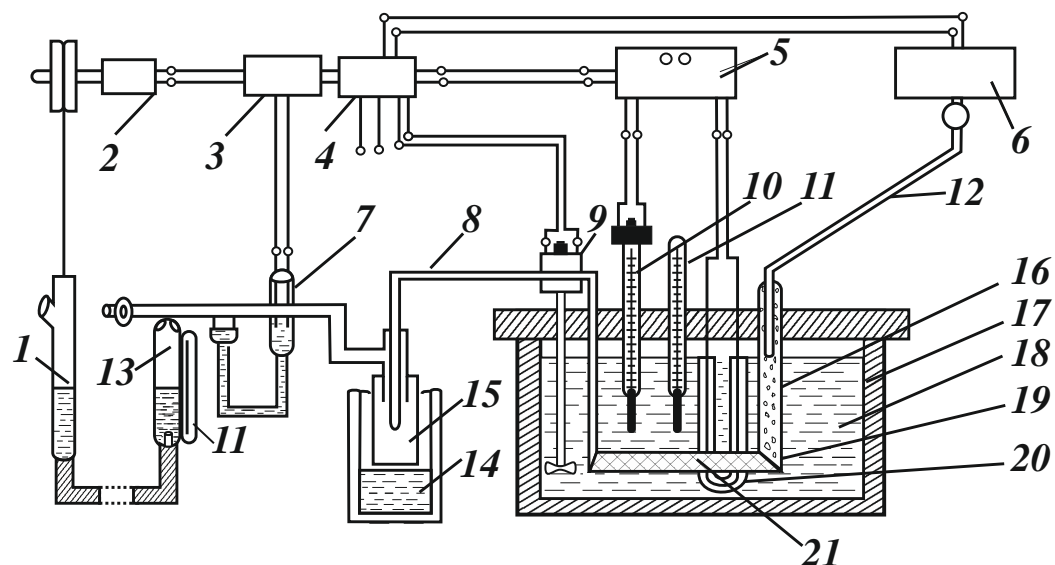


**FIGURE 1.** Apparatus for studying chemical equilibria in a dynamic flow system: 1, counterpoise flask, 2, electric motor, 3, controller, 4, control panel, 5, thyristor relay, 6, dosing pump, 7, electrolytic cell, 8, outlet capillary, 9, stirrer, 10, controlling thermometer, 11, thermometers, 12, inlet capillary, 13, gas collector, 14, Dewar bottle, 15, condensate collector, 16, crushed glass filler, 17, thermostat jacket, 18, oil, 19, reactor, 20, heater, 21, catalyst area [7].

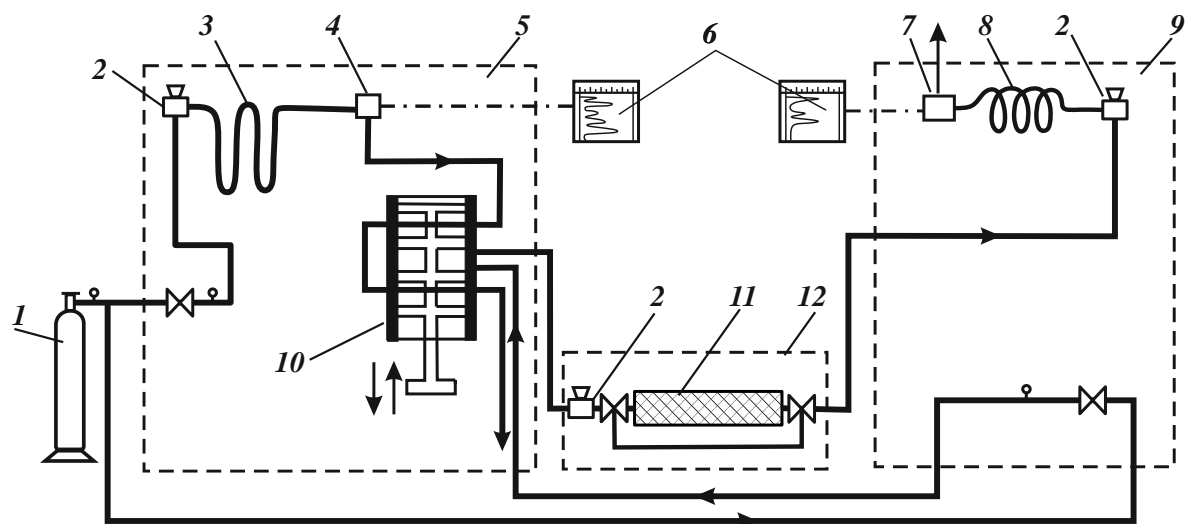


**FIGURE 2.** Pulse chromatographic apparatus for studying chemical equilibria: 1, gas carrier vessel, 2, liquid sample vaporizer, 3, packed chromatographic column, 4, thermal conductivity detector, 5, preparation section, 6, potentiometric recorders, 7, flame ionization detector, 8, capillary chromatographic column, 9, analytical section, 10, gas flow switch, 11, microreactor, 12, microreactor section [7].

Chemical equilibria for the following reaction types and compound classes were systematically studied: dehydrogenation of cyclohexanol [9], cyclopentanol [10], and methylcyclohexanols [9]; dehydrohalogenation of 2-chloropropane [11], chlorocyclohexane [12], and chlorocyclopentane; and isomerization of alkanes  $C_6H_{14}$  to  $C_8H_{18}$  [13, 14], cyclohexane = methylcyclopentane [15], alkenes  $C_5H_{10}$  to  $C_7H_{14}$  [16, 17, 18, 19, 20], methylcyclopentenenes  $C_6H_{10}$  [21], methylcyclohexenes  $C_7H_{12}$  [22], hexadienes  $C_6H_{10}$  [23, 24], chloroalkanes  $C_3H_7Cl$  to  $C_{10}H_{21}Cl$  [20, 25, 26, 27, 28, 29], diastereomers of alcohols including methylcyclohexanols, menthol, borneol [30], *etc.*

The results of the isomerization studies together with similar results available in the literature are summarized in a reference book published originally in 1988 [31] and translated into English in 1992 [32].

## 2.2. Static bomb combustion calorimeters

Two static bomb combustion calorimeters were used by our group for studying substances of general formula  $C_nH_mO_kN_l$ .

### Bomb calorimeter V-08E [6]

This calorimeter was a customized version of the commercially manufactured V-08 calorimeter with a bomb volume of about  $330 \text{ cm}^3$  and an energy equivalent close to  $14700 \text{ J}\cdot\text{K}^{-1}$ . We added an electronic temperature controller, an ignition control system, and a temperature data acquisition unit. The relative standard uncertainty of the instrument was estimated from the standard deviation of the mean in the experiments with benzoic acid to be  $1.0\cdot 10^{-4}$  [33].

### Bomb calorimeter KS-95 [34]

This calorimeter was designed and built to measure energies of combustion for small samples, with a useful range of (0.05 to 0.5) g in mass. Its calorimetric bomb had a small volume ( $95 \text{ cm}^3$ ) and a constant-temperature air bath. Schematic representation of this calorimeter is shown in figure 3. The calorimetric bomb was suspended from a metal rod used in the ignition system. A Dewar bottle of about  $2500 \text{ cm}^3$  volume was used as a calorimetric vessel. The bath temperature was controlled with a proportional-integral-differential algorithm assuring temperature control with a tolerance of  $\pm 0.01 \text{ K}$ . The calorimeter constant was close to  $9830 \text{ J}\cdot\text{K}^{-1}$ , and the relative standard uncertainty of the instrument was found to be  $2.5\cdot 10^{-4}$  [34].

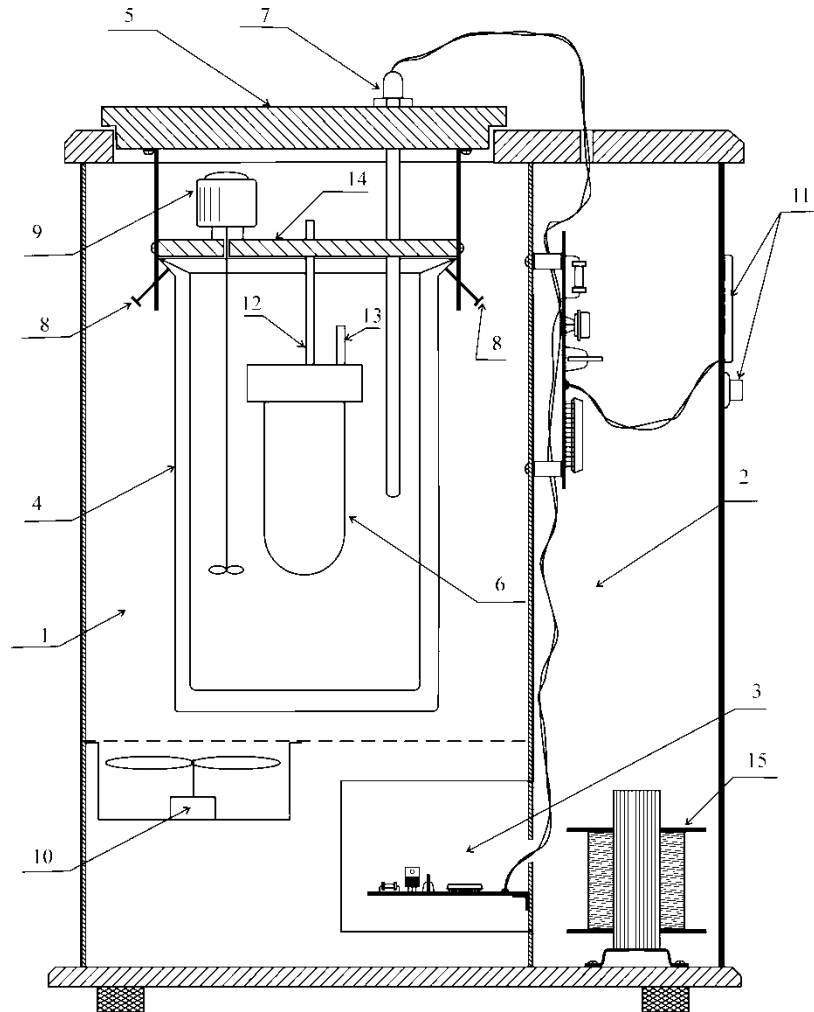


**FIGURE 3.** Schematic representation of the static bomb calorimeter of combustion KS-95: 1, constant-temperature air bath, 2, compartment for the electronic control system, 3, thermostatted compartment for the analog-digital converter, 4, calorimetric vessel, 5, cover of the constant-temperature air bath, 6, calorimetric bomb, 7, platinum resistance thermometer, 8, screws securing calorimetric vessel, 9, electric motor of calorimetric vessel stirrer, 10, electric motor of stirrer of air bath, 11, control panel, 12, rod suspending the calorimetric bomb and used in the ignition system, 13, second electrode used in the ignition system, 14, calorimetric vessel cover, 15, power supply transformer [34].

### *2.3. Calorimeters to measure heat capacities and enthalpies of phase transitions*

Four calorimeters used by our group (TAU-1, TAU-10, TM-2, and SK-1) for high precision measurements of heat capacities and enthalpies of phase transitions provided a unique opportunity to conduct these measurements over a temperature range from (5 to 700) K.

#### Adiabatic calorimeters TAU-1 and TAU-10 (BKT-3)

Two small volume calorimeters [35], TAU-1 and TAU-10, were commercially sourced from VNIIFTRI (Russia) and were used to measure heat capacities and enthalpies of phase transitions in the temperature range of (5 to 320) K and (5 to 370) K, respectively. We developed software to support experimental data analysis including heat capacity polynomial interpolation, calculation of enthalpies of phase transitions, purity determination with the fractional-melting technique, and calculation of smoothed heat capacities and derived functions. At  $T > 40$  K, the expanded uncertainty was found to be  $4 \cdot 10^{-3} C_p$  [6, 36].

#### Scanning calorimeter of a heat-bridge type TM-2 [6]

This calorimeter (figure 4) was designed and built in our laboratory by engineer Evgeny N. Kozyrsky. The use of two measuring cells, one with a studied sample and the other with a reference sample, made it possible to conduct heat-capacity measurements in the temperature range of (250 to 650) K based on the equation:

$$C_P = A(T)(U_x / U_s) - B(T) \quad (2)$$

where  $U_x$  and  $U_s$  are voltages of thermocouples used in the sample cell  $x$  and in the reference cell  $s$ ,  $A(T)$  and  $B(T)$  are calibration parameters. We showed that the reduction in heat-adsorbing surfaces and stronger thermocouple signals results in higher repeatability of the heat-capacity measurements for the two-cell calorimeter in comparison with the triple heat bridge apparatus [37].

Also, we demonstrated that reflective properties of the cell surface should be kept as constant as possible to obtain the best results.

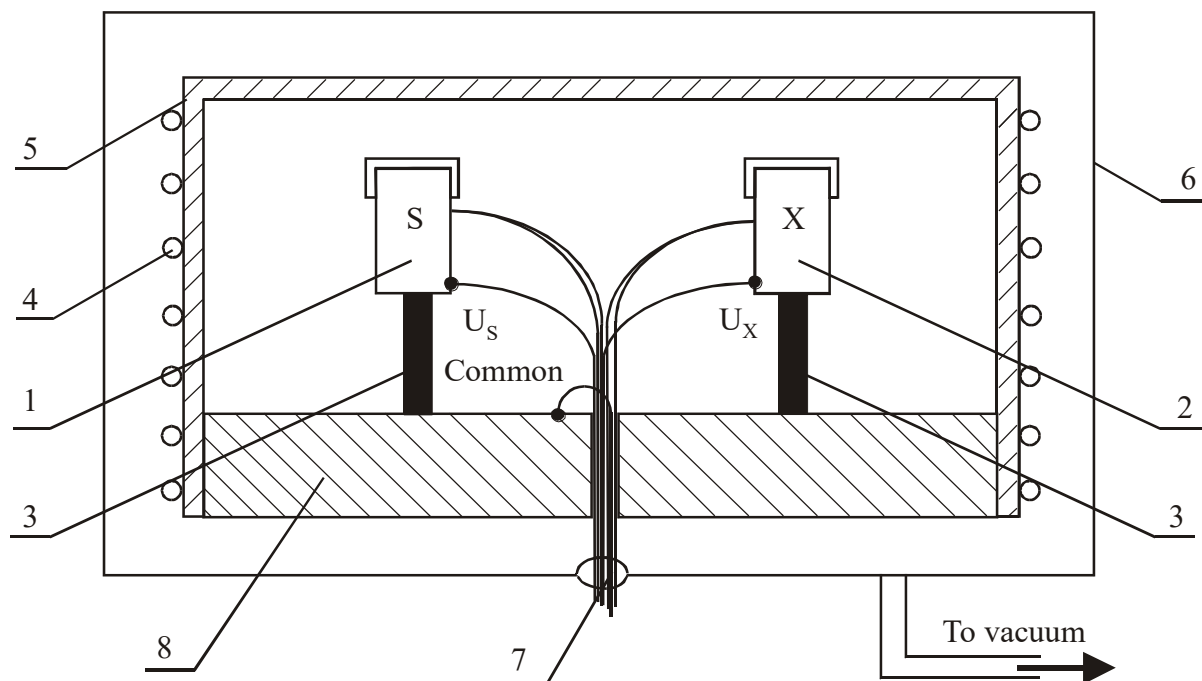


**FIGURE 4.** Differential scanning calorimeter of a heat-bridge type: 1, reference cell, 2, sample cell, 3, Constantan rods, 4, heater, 5, cover, 6, stainless steel shield, 7, thermocouples, 8, copper heater block [6].

#### Single-cell scanning calorimeter SK-1

This instrument was designed and built to measure heat capacities and enthalpies of phase transitions in the temperature range of (300 to 700) K (figure 5) for samples of a (0.1 to 0.5) g mass. The control system and software, developed in-house, allowed for heating rates of (0.1 to 4)  $\text{K}\cdot\text{min}^{-1}$ , as well as on-going testing, automated corrections for baseline drift, and smoothing experimental results.

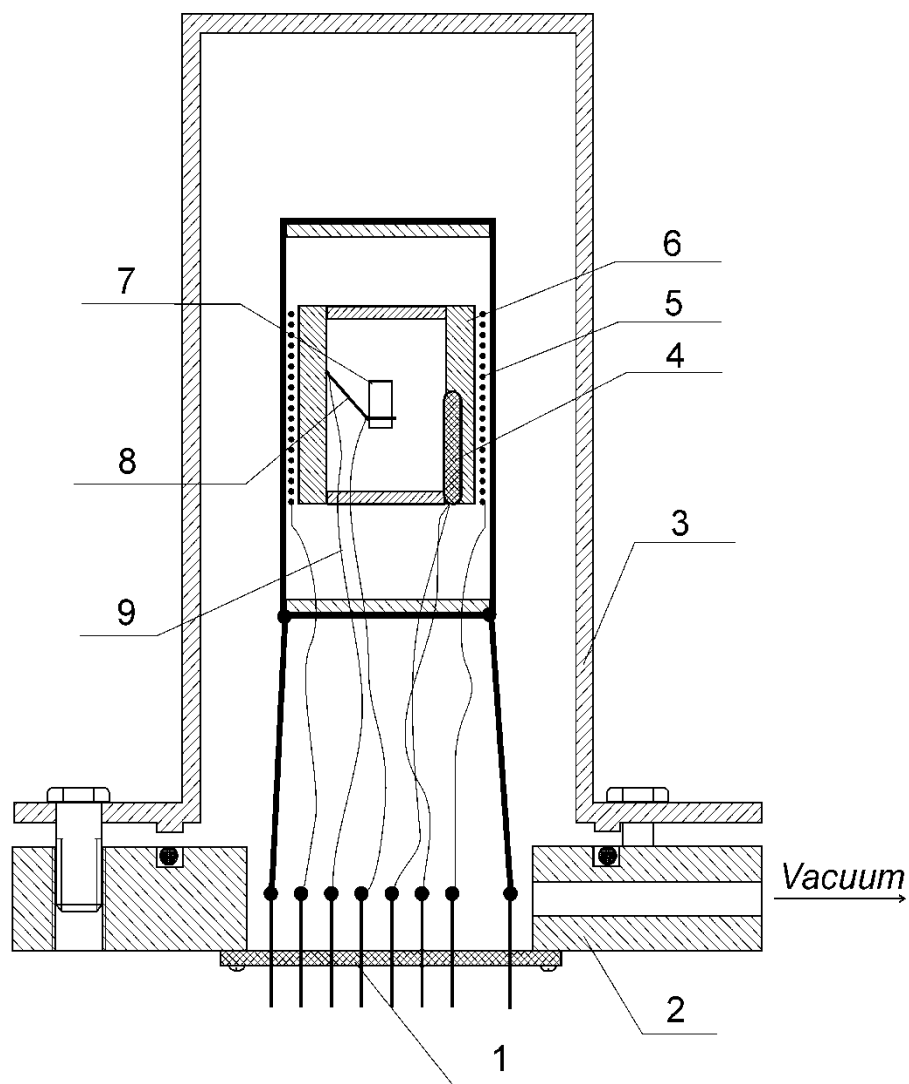


**FIGURE 5.** Single-cell scanning calorimeter SK-1: 1, pin and socket connector, 2, calorimeter base, 3, vacuumed jacket, 4, platinum resistance thermometer, 5, jacket heater, 6, calorimetric jacket, 7, ampoule with a sample, 8, sample holder made of Chromel, 9, thermocouple wire (Copel).

#### 2.4. Calvet-type differential heat flux microcalorimeter

A commercial solution microcalorimeter MID-200 was redesigned to measure enthalpies of vaporization and sublimation [38]. Special calorimetric cells were designed and built by Viktor M. Sevruk (figure 6).

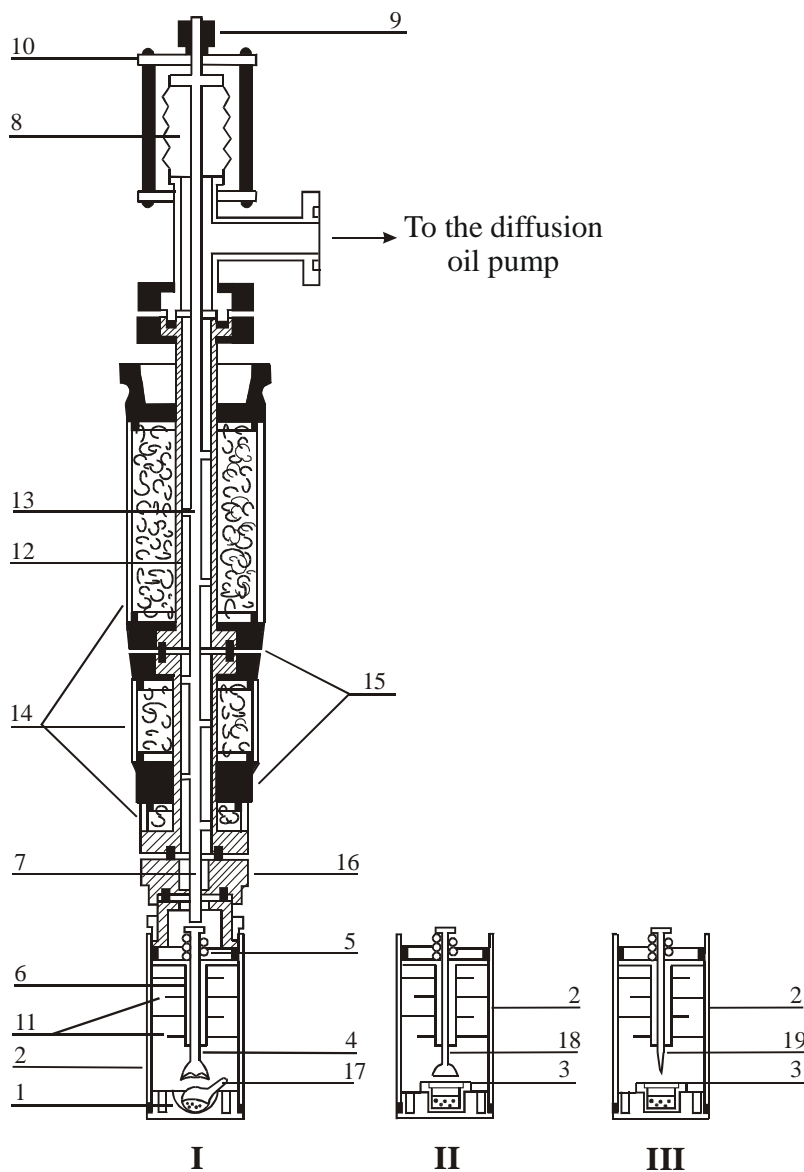


**FIGURE 6.** Calorimetric cell for a differential heat flux calorimeter: 1, the lower lid, 2, evaporation chamber, 3, effusion cell with a sample, 4, metal rod, 5, spring, 6, directing channel,

7, subsidiary rod, 8, bellows, 9, fixing screw, 10, limiting strap, 11, metal shields, 12, Teflon tube, 13, segmental shields, 14, thermoinsulating coats, 15 and 16, metal contacts for thermostating, 17, glass cell, 18, metal rod with a seal band, 19, metal rod with a spire, I, evaporation chamber with crushed ampoule, II, evaporation chamber with an effusion cell closed by a metal rod, III, evaporation chamber with an effusion cell obtained by piercing the membrane [38].

The enthalpies of vaporization (sublimation),  $\Delta_{\text{vap(sub)}}H$ , were determined as follows:

$$\Delta_{\text{vap(sub)}}H = K \int_0^{\tau} \Delta E(\tau) dT \quad (3)$$

where  $\Delta E$  is the voltage corresponding to the temperature difference between the calorimetric cell and the heat-conductive thermostatted shell, and  $K$  is the coefficient determined during a calibration using reference materials such as water, naphthalene, or benzoic acid. The relative standard uncertainty for the enthalpies of vaporization or sublimation was close to  $5 \cdot 10^{-3}$ .

### 2.5. Determination of vapor pressure by the Knudsen effusion method [6]

The vapor pressure of a variety of substances was measured by the Knudsen effusion method with the use of two apparatuses designed and built in our laboratory. These instruments, similar in overall design, had different thermostats. The low-temperature apparatus (figure 7) used a liquid thermostat and allowed the measurements to be conducted in the range  $T = (243 \text{ to } 358) \text{ K}$ . In the high-temperature apparatus, the effusion cell was inserted into a thermostating block made of copper, yielding a working range of  $T = (308 \text{ to } 530) \text{ K}$ . The vapor pressure was calculated with the equation:

$$p_s = \frac{\Delta m}{KS\tau} \sqrt{\frac{2\pi RT}{M}}, \quad (4)$$

where  $\Delta m$  is the sample mass loss during exposure time  $\tau$ ,  $S$  is the orifice surface area,  $M$  is the molar mass of a vapor, and  $K$  is the Clausing coefficient. For crystalline samples, the condensation coefficient was also considered. We introduced corrections associated with the sample mass loss  $\Delta m_n$  and time  $\Delta \tau_n$  under non-stationary conditions. Anisotropy of a gas in the Knudsen cell was considered [39, 40], which made it possible to extend an upper limit of the measurable vapor pressure to 70 Pa. To measure the vapor pressure over crystals, we used special cells with the enlarged contact surface area, maximizing heat transfer with the sample.

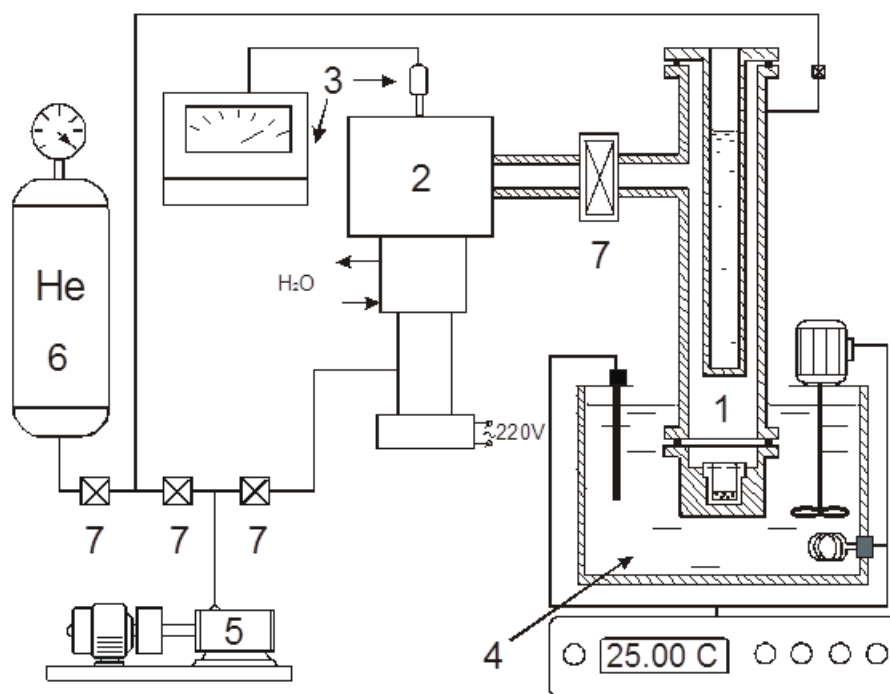


**FIGURE 7.** Apparatus for vapor pressure determination by the integral effusion Knudsen method: 1, measuring unit (effusion cell with a sample, system connecting to vacuum, liquid nitrogen trap), 2, oil diffusion pump, 3, vacuum meter with thermocouple vacuum metering lamp, 4, liquid thermostat, 5, rotary vane vacuum pump, 6, helium vessel, 7, bellows vacuum switches [6].

A combination of the experimental apparatuses described in sections 2.1 to 2.5 provided the unique capabilities of determining heat capacities, vapor pressures, enthalpies of formation, and derived properties in the crystal, liquid (glass), and gas phases.

### 3. Thermodynamic properties and molecular structure

#### 3.1. Modeling and prediction of thermodynamic properties based upon classical theory of molecular structure

We discovered great benefit from exploring the relationship between thermodynamic properties and molecular structure. In particular, leveraging the classical theory of molecular structure and the principles suggested by Tatevsky [5], we developed efficient methods for property prediction.

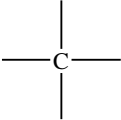
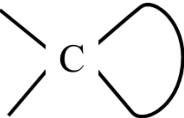
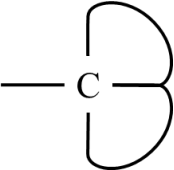
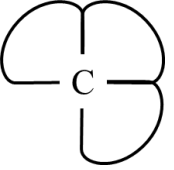
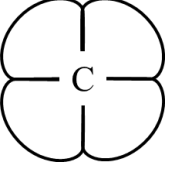
In these methods, property  $P$  can be presented as a sum:

$$P = \sum_{a_i} P_{a_i} + \sum_{a_i-a_j} P_{a_i-a_j} + \sum_{a_i \leftrightarrow a_j} P_{a_i \leftrightarrow a_j} \quad (5)$$

where  $P_{a_i}$ ,  $P_{a_i-a_j}$  and  $P_{a_i \leftrightarrow a_j}$  are partial properties associated with effective atom  $a_i$ , effective bond  $a_i-a_j$ , and interaction of chemically non-bonded atoms  $a_i \leftrightarrow a_j$ . Tatevsky distinguished effective atoms by their chemical nature, valence state, and environment. We suggested adding “cyclicity” as an identifying factor for effective atoms [41] and demonstrated [7, 8, 41] that six types of effective carbon atoms can be identified by considering their cyclicity (Table 1). Superscripted indexes ( $C^I$ ,  $C^{II}$ ,  $C^{III}$ ,  $C^{IV}$ ,  $S-C^I$ ,  $C^{II} \geq 2$ ) characterize the size of the ring containing the carbon atom. For example,  $C^I = 2$  corresponds to a double bond while  $C^I = 2$ ,  $C^{II} = 2$  corresponds to a triple bond.

**TABLE 1**

Types of effective atoms considering their cyclicity

| Type        | Abbreviation                       | Structure   |
|-------------|------------------------------------|---|
| Acyclic     | $C$                                |    |
| Monocyclic  | $C^{C^I}$                          |    |
| Bicyclic    | $C^{C^I, C^{II}}$                  |    |
| Tricyclic   | $C^{C^I, C^{II}, C^{III}}$         |   |
| Tetracyclic | $C^{C^I, C^{II}, C^{III}, C^{IV}}$ |  |
| Spiro       | $C^{S-C^I, C^{II}}$                |  |

Addition of the cyclicity parameter allowed for uniform classification of atom types in cyclic compounds. This significantly expanded possibilities of additivity-based (group-contribution) methods for property prediction. Grikina and Tatevsky independently made a similar conclusion [42]. Applying such modeling methods to physical and chemical properties yielded a foundation for addressing a wide range of challenges based upon classical theory [7]. Example applications

include planning experiments, evaluating self-consistency testing of experimental data, predicting properties of substances lacking in experimental data, and detecting compounds that display anomalous behaviors.

For polyfunctional compounds, we developed prediction schemes that reduced the number of parameters without compromising the fidelity of the model. One particularly powerful approach [7, 43, 44, 45, 46] is based on incremental substitutions  $RH \rightarrow RX$ , where X represents, for example,  $CH_3$ , halogens, or OH. Normal alkanes were selected as the reference series for acyclic saturated compounds. The substitutional groups were subdivided into primary, secondary, tertiary, and quaternary. In addition, interactions between the substituent (X) and other non-hydrogen atoms located in positions 1 and 4 relative to each other were taken into account. Thus, the enthalpy of formation of the compound RX can be predicted as follows:

$$\Delta_f H(RX) = \Delta_f H(n-C_nH_{2n+2}) + \sum_i l_i \Delta_f H(X) + \sum_j \sum_{k \geq j} m_{jk} \beta_{1 \leftrightarrow 4}(X_j \leftrightarrow X_k) \quad (6)$$

The results from this methodology are independent of the order of substitutions. Moreover, when comparing this approach to one based on classification of effective bonds, reliability in prediction of enthalpies of formation in the gas and liquid phases is comparable even while the number of required parameters is halved [42, 44].

In many instances, physical justification of the additivity-based (group-contribution) methods is not straightforward. Indeed, it was shown [46] that the partition function

$$Q = \sum_i e^{-\varepsilon_i / kT} \quad (7)$$

and, correspondingly, thermodynamic properties that depend on it ( $C_p$ ,  $S^\circ$ , *etc.*) are not additive. However, the fact that these properties do tend to exhibit additive behavior results from mutual cancellation of non-additivity effects for transitional, rotational, and vibrational contributions. We



**TABLE 2**

Types and subtypes of structural isomerization reactions and molecular structure changes

| Isomerization type | Isomerization subtype           | Change         |                   |        |
|--------------------|---------------------------------|----------------|-------------------|--------|
|                    |                                 | Chemical bonds | First environment | Cyclic |
| Positional         | Isomers of the same family      | -              | -                 | -      |
|                    | Isomers of different families   | -              | +                 | -      |
| Cyclic             | With the ring size change       | -              | +                 | +      |
|                    | With change of ring attachments | -              | +                 | +      |
| Functional         | Non-valent                      | +              | +                 | -      |
|                    | Cyclic                          | +              | +                 | +      |
|                    | Valent                          | +              | +                 | +      |

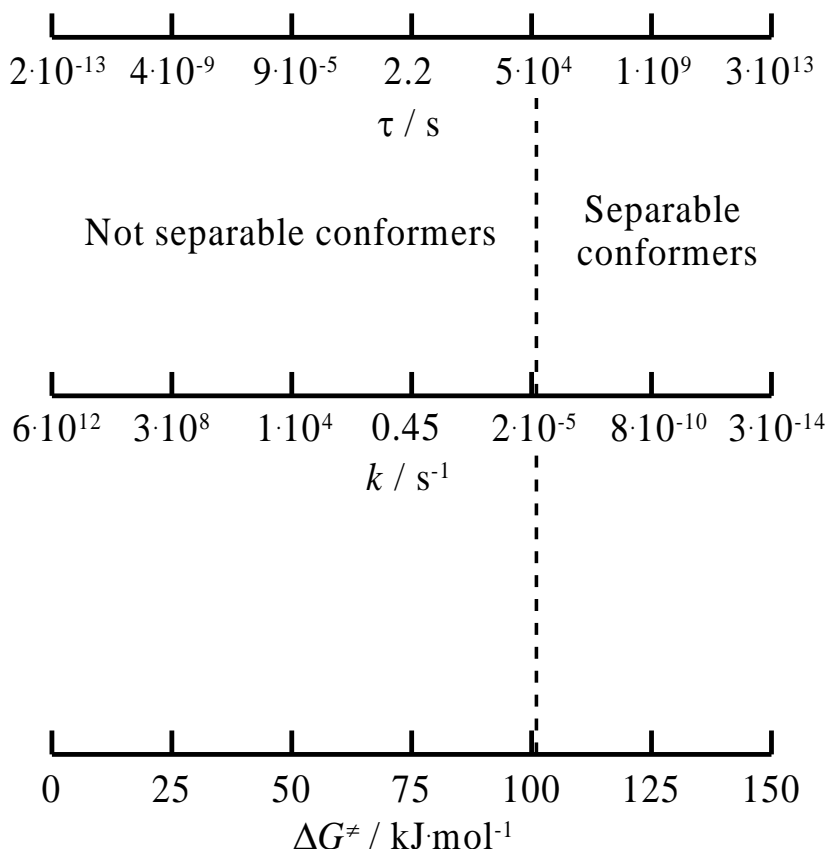


**FIGURE 8.** Activation scale of conformational transformations at  $T = 298$  K.  $k$  is a reaction rate constant, calculated as  $k = (k_B T/h)\exp(-\Delta G^\ddagger/RT)$ ,  $\tau$  is an average lifetime,  $\tau = 1/k$ . Reproduced from Ref. [48] with permission from the Royal Society of Chemistry.

Following van der Waals' principles of defining a "pure substance" from a thermodynamic standpoint [49], one can distinguish:

1) Pure substances, for which melting and normal boiling temperatures are constant, although their equation of state might be complex. Such systems will have a logarithmic contribution caused by the mixing of different molecules:

$$\Delta_{\text{mix}}S = -R\sum_i x_i \ln x_i \quad (8)$$

2) "Thermodynamic individuals" for which the entropy does not have a mixing contribution.

3) “Molecular individuals” characterized by a unique molecular structure.

This system can be further expanded to take advantage of a detailed understanding of molecular structure, allowing us to distinguish five categories of substances [8]:

- 1) isomerically pure substances consisting of molecules with the same atomic composition;
- 2) structurally pure substances consisting of molecules of the same structure but having a variety of conformational and configurational species.
- 3) configurationally pure substances consisting of either achiral or chiral but configurationally identical molecules;
- 4) conformationally pure substances consisting of molecules of the same conformation due to structural, thermodynamic, or kinetic limits to form conformational mixtures;
- 5) individual substances consisting of molecules with a single possible configuration.

Ideal-gas thermodynamic properties of conformational mixtures can be represented as [50]:

$$S^{\circ} = \sum_{i=1}^n x_i S_i^{\circ} + S_{\text{conf}}^{\circ} = \sum_{i=1}^n x_i S_i^{\circ} - R \sum_{i=1}^n x_i \ln x_i, \quad (9)$$

$$C_p^{\circ} = \sum_{i=1}^n x_i C_{p,i}^{\circ} + C_{p,\text{conf}}^{\circ} = \sum_{i=1}^n x_i C_{p,i}^{\circ} + \frac{1}{RT^2} \sum_{i=1}^n x_i \sum_{j>1}^n x_j (\Delta H_{ij}^{\circ})^2, \quad (10)$$

$$\frac{H^{\circ}(T) - H^{\circ}(0)}{T} = \sum_{i=1}^n x_i \frac{H_i^{\circ}(T) - H_i^{\circ}(0)}{T} + \Delta H_{\text{conf}}^{\circ} = \sum_{i=1}^n x_i \frac{H_i^{\circ}(T) - H_i^{\circ}(0)}{T} + \sum_{i=2}^n x_i \frac{\Delta H_{1i}^{\circ}}{T}, \quad (11)$$

where  $x_i$  is the equilibrium mole fraction of the  $i$ th conformer and  $\Delta H_{ij}^{\circ}$  is the enthalpy difference between the  $i$ th and  $j$ th conformers. Conformational contributions to entropy and heat capacity as a function of temperature and the enthalpy difference for mixtures containing three and six conformers are shown in figure 9.

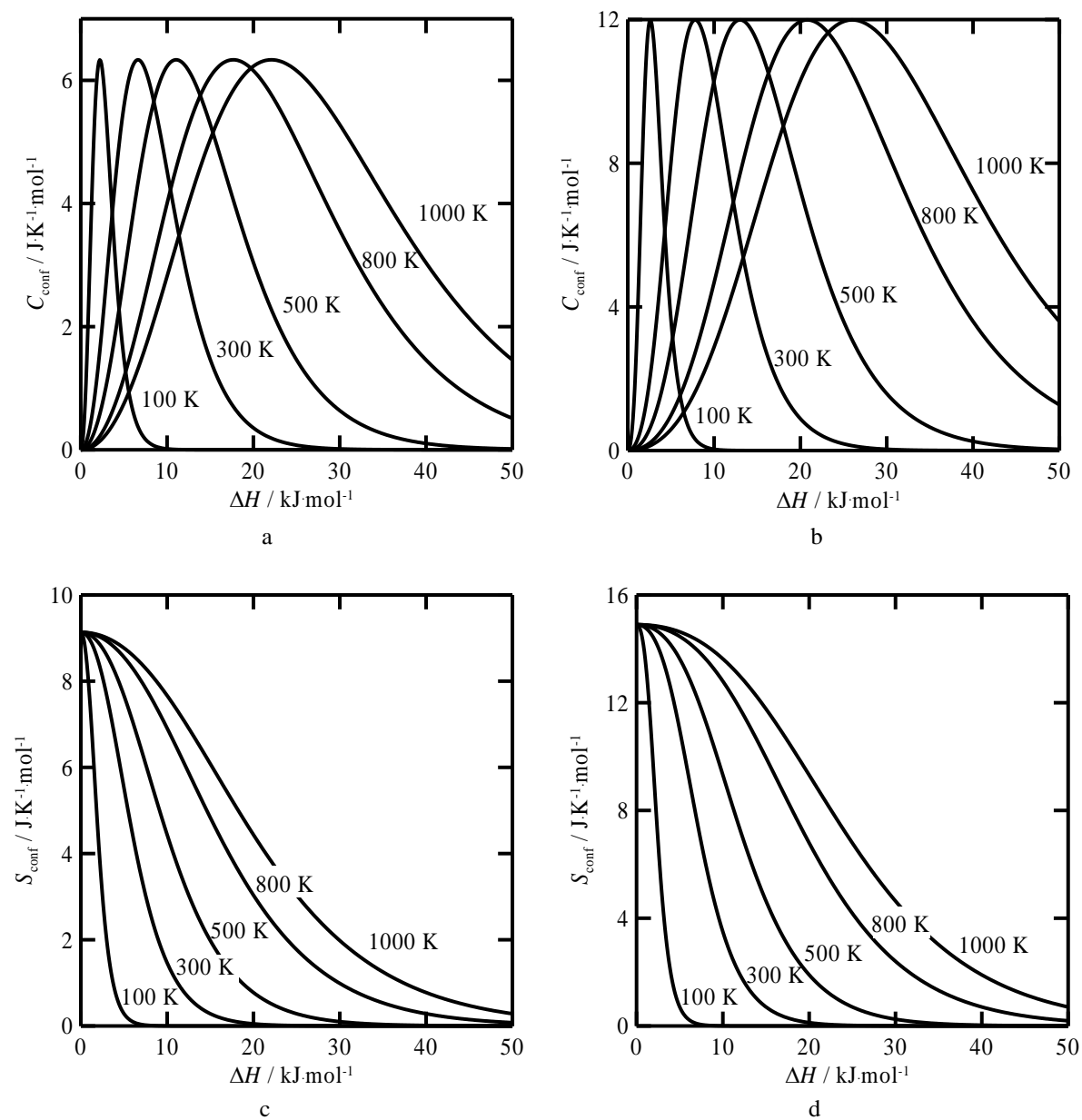


**FIGURE 9.** Conformational contribution to heat capacity and entropy for the systems: (a) and (c), one most stable conformer and two conformers of relative enthalpy  $\Delta H$ ; (b) and (d), one most stable conformer and five conformers of relative enthalpy  $\Delta H$ . Reproduced from Ref. [48] with permission from the Royal Society of Chemistry.

### 3.3. Calculation of thermodynamic properties with statistical thermodynamics

Statistical thermodynamics makes it possible to extrapolate thermodynamic properties over a broad range of temperatures and to establish a relationship between molecular structure and macroscopic thermodynamic properties. For an ideal gas, the entropy is presented as a sum of contributions corresponding to various degrees of molecular freedom (translation, overall rotation, vibration, internal rotation, and electronic) [51]:

$$S(T, P) = S_{\text{tr}}(T, P) + S_{\text{rot}}(T) + S_{\text{vib}}(T) + S_{\text{int.rot}}(T) + S_{\text{e}}(T) \quad (12)$$

These contributions, in turn, depend on molecular parameters such as the molar mass,  $M$ , the product of moments of inertia,  $I_A I_B I_C$ , the symmetry number,  $\sigma$ , the frequencies of normal modes,  $\nu_i$ ; potential functions,  $V(\varphi)$ , and reduced moments of inertia,  $I_r$ , of internal rotation, and energies of electronic levels of a molecule. To determine the entropy and other thermodynamic properties of gases, one requires detailed information about the structure and energy states of the molecule. We demonstrated [52] that calculations of thermodynamic properties using methods of statistical thermodynamics can be performed reliably even in the situations when there was no reliable experimental data related to molecular structure parameters. Such situations are rather common because either the targeted substances cannot be synthesized, or the synthesized samples cannot be purified enough for reliable experimental measurements. Under those circumstances we performed calculations of thermodynamic properties using algorithms illustrated in figures 10 and 11. These algorithms include the use of quantum chemical procedures for determination of the geometric parameters, the normal vibration frequencies, the potential barriers of internal rotation and of ring inversion, and the energy states of the molecule of interest.

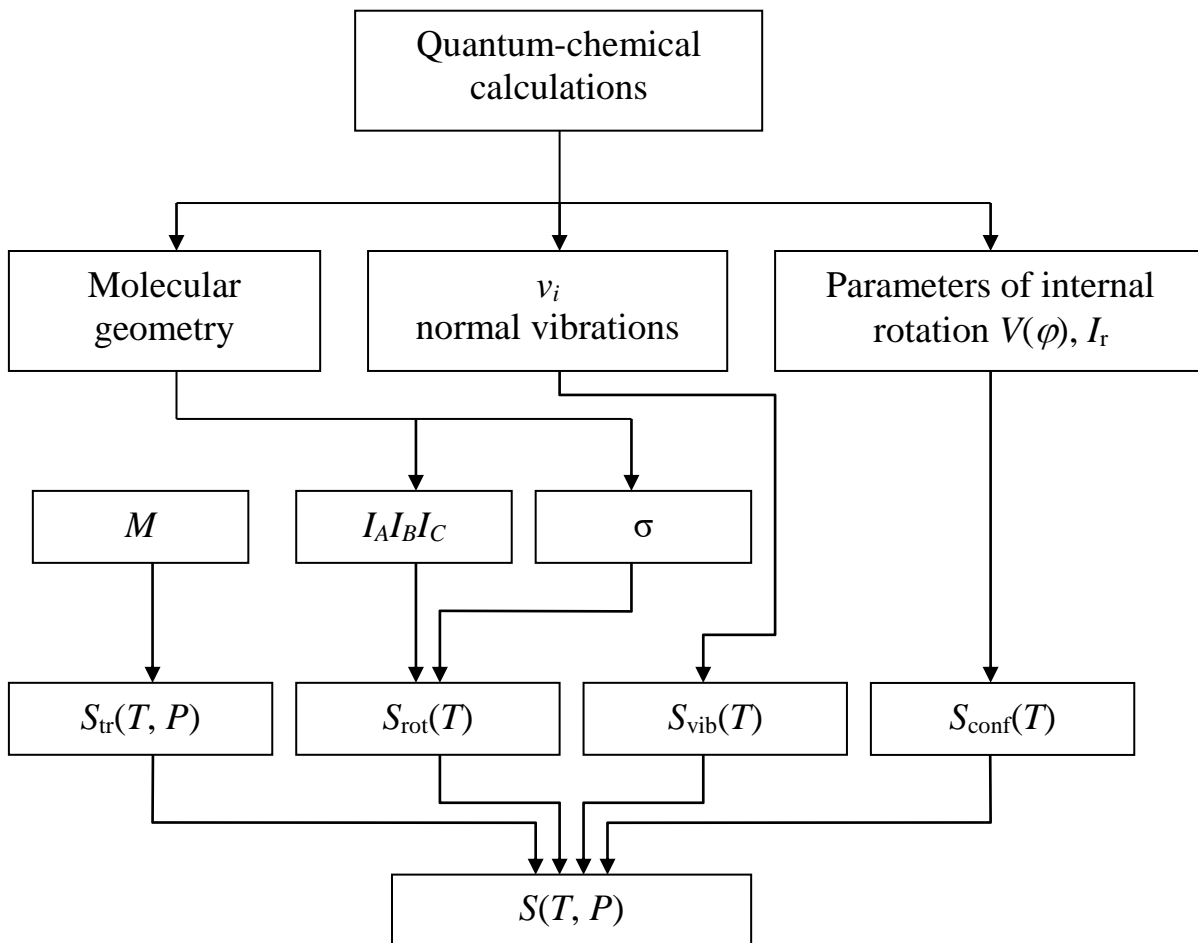


**FIGURE 10.** Principal algorithm of statistical thermodynamics calculations of ideal-gas entropy.

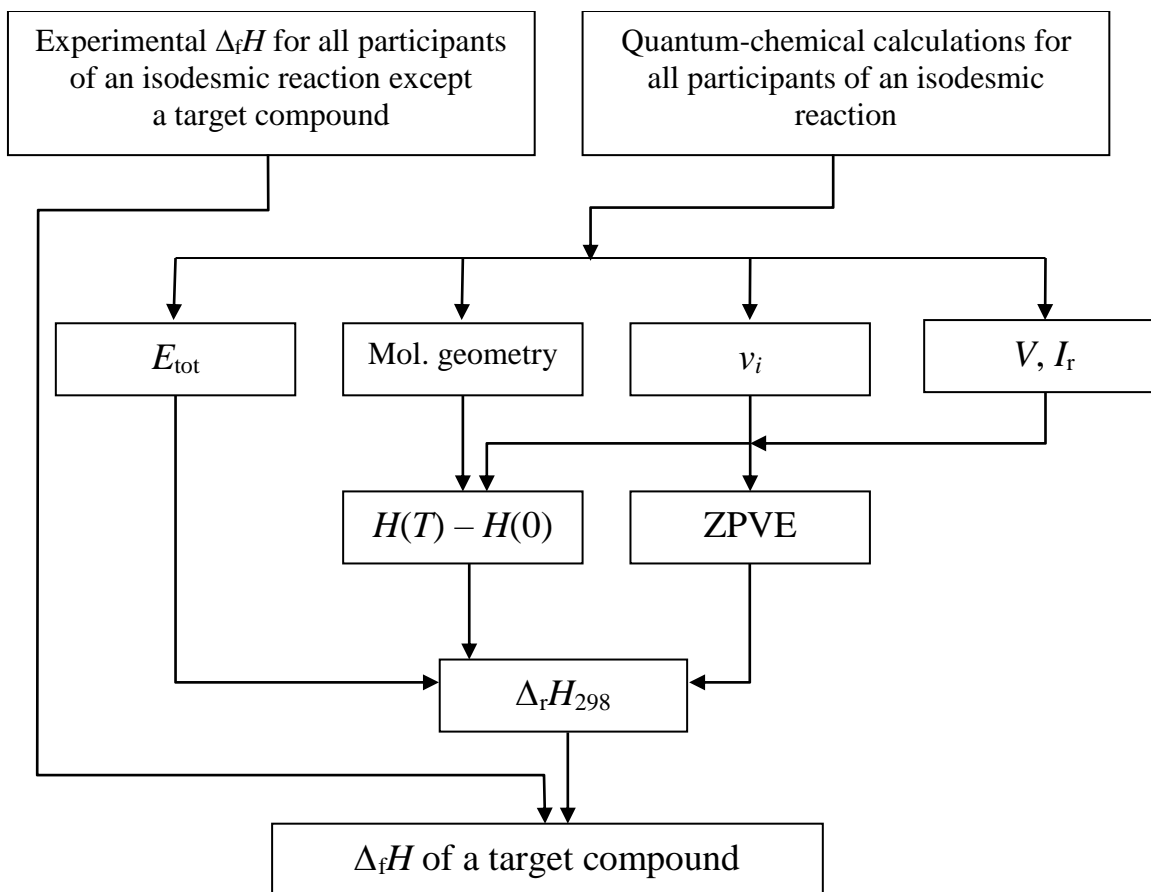
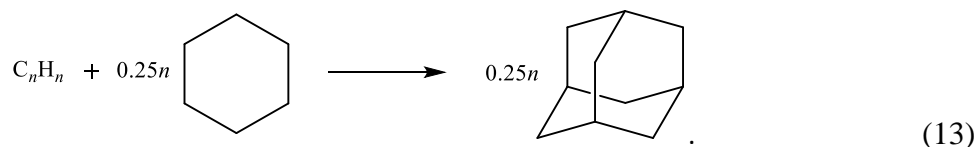


**FIGURE 11.** Principal algorithm of the  $\Delta_f H$  calculation using quantum-chemical methods and the isodesmic reactions concept.

We used these algorithms in a systematic study of the thermodynamic properties of polyhedranes,  $C_n H_n$  [53], including Platonic polyhedron structures such as tetrahedrane,  $C_4 H_4$ , cubane,  $C_8 H_8$ , and dodecahedrane,  $C_{20} H_{20}$ ; truncated Platonic polyhedron structures including truncated tetrahedrane,  $C_{12} H_{12}$ , truncated octahedrane,  $C_{24} H_{24}$ , truncated cubane,  $C_{24} H_{24}$ , truncated icosahedrane,  $C_{60} H_{60}$ , and prismanes,  $C_{10} H_{10}$ ,  $C_{12} H_{12}$ ,  $C_{14} H_{14}$ , and  $C_{16} H_{16}$ . The results of our experimental measurements of the thermodynamic properties of cage hydrocarbons confirmed the above statistical mechanical procedures in the combined temperature range of (5 to 530) K including adamantane,  $C_{10} H_{16}$  [54,

55], 1,1-diadamantane  $C_{20}H_{30}$  [56]; heptacyclotetradecane  $C_{14}H_{16}$  [57], and pentacycloundecane  $C_{11}H_{14}$  [58]. For calculations of the enthalpies of formation of hydrocarbons  $C_nH_n$ , we used the following isodesmic reaction:



Having identified limits for the use of classical approaches for determining the internal rotation contributions as a function of a potential barrier and a statistical sum of a free rotor [51, 59, 60], we developed new procedures for statistical calculations of the ideal-gas thermodynamic properties for such molecules. We proposed a new method for estimation of the reduced moment of inertia for pseudorotation in a cyclopentane ring [61]. We established that one can use equations (9) to (11) to calculate contributions of intramolecular transformations based on energy differences of conformers  $\Delta H_{ij}$  and their equilibrium compositions  $x_i$  [50].

### *3.4. Determination of structural parameters of molecules using methods of statistical thermodynamics*

Pitzer [2] first demonstrated the power of statistical thermodynamics in determining structural parameters of molecules based on enforcing consistency between the calculated and experimentally derived values of entropy,  $S^\circ$ , and heat capacity,  $C_p$ , in an ideal gas. As a part of this development, the concept of hindered internal rotation was established, and the value of the potential barrier of internal rotation in ethane was determined. The presence of free pseudorotation in cyclopentane and ring inversion in cyclohexane derivatives was also demonstrated [2].

Following this approach, we estimated conformational and tautomeric (isomeric) compositions for substituted derivatives of cyclohexane and cyclopentane [62, 63, 64], tetrazole [65, 66], parabanic

and barbituric acids [67, 68], fullerene hydrides ( $C_{60}H_n$ ,  $n = 2, 4, 8, 18,$  and  $36$ ) [52, 53] as well as had determined the parameters of molecular models. These results allowed us to reach excellent consistency in entropy for other compounds [34, 55, 69, 70, 71, 72, 73].

#### 4. Thermodynamic properties, phase states, and their structures

##### 4.1. Discreteness of thermodynamic properties of substances at phase transitions and at a glass transition

Thermodynamic properties change discretely at the transitions crystal (glass)  $\rightarrow$  liquid  $\rightarrow$  gas (figure 12), following these trends:

1. Normally, heat capacities of organic liquids are greater than those of the crystal and gas phases for the same substance at the same temperature  $T$ , although for the entropies,  $S_{cr}^\circ(T) < S_l^\circ(T) < S_g^\circ(T)$ .
2. Heat capacity of a liquid is higher than that of a glass even though the structures and entropies of a glass and a supercooled liquid at  $T \rightarrow T_g$  are identical.
3. Coefficients of thermal expansion  $\alpha_p$  for liquids are significantly higher than those for crystals.

We used a type of lattice model called a hole model to describe the heat capacity changes at the glass transition and fusion. In this model, the liquid volume  $V$  is divided into cells of equal volume  $v_0$ . Then,

$$V = v_0(N_0 + N_1 r) \quad (14)$$

where  $N_0$  and  $N_1$  are the numbers of empty cells (holes) and molecules, respectively, and  $r$  is the number of cells occupied by a molecule. Thermal expansion of a liquid is assumed to be caused by increasing  $v_0$  due to anharmonicity of vibrations and  $N_0$ . The latter explains the higher thermal expansion coefficients and heat capacity of the liquid relative to the glass or crystal.

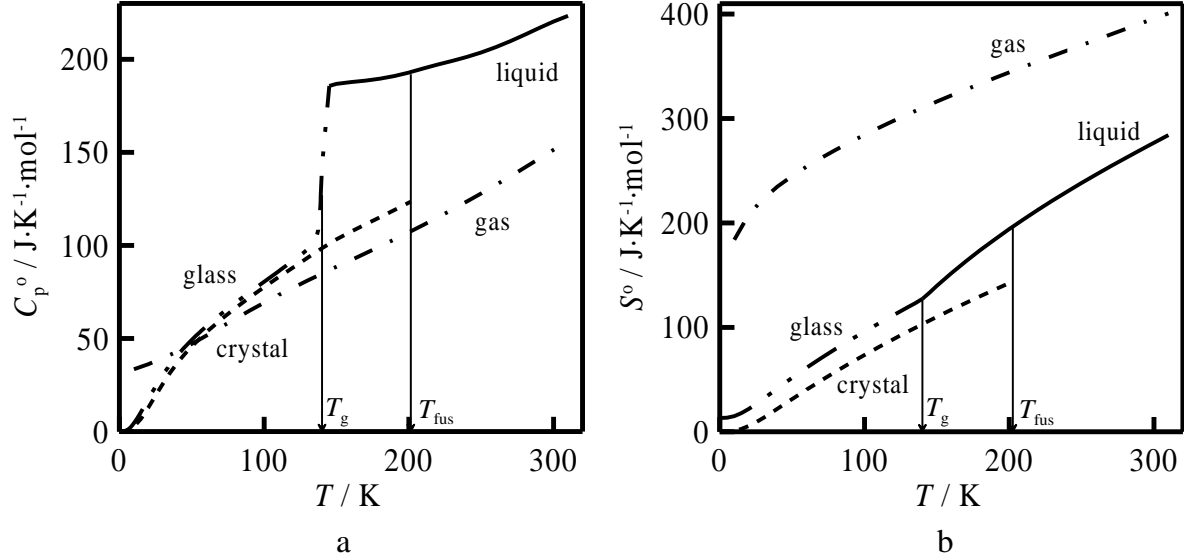


**FIGURE 12.** Heat capacity (a) and entropy (b) for different phases of cyclohexyl formate. Reproduced from Ref. [48] with permission from the Royal Society of Chemistry.

Following DiMarzio and Dowell [74], we assumed that

$$\Delta_{\text{gl}}^1 C_p = \Delta C_{\text{conf}} + \Delta C_{\text{vib}} + C_h \quad (15)$$

where  $\Delta C_{\text{conf}}$  is the conformational contribution to the liquid heat capacity,  $C_h$  is the hole contribution caused by the change in the number of empty cells in the liquid with temperature, and  $\Delta C_{\text{vib}}$  is a contribution related to changes in temperature dependences of vibrational frequencies while transforming from glass to liquid. The conformational contribution appears because the conformational transformations, frozen in the glass, are allowed in the liquid phase. This contribution was found from the equation:

$$\Delta C_{\text{conf}} = \frac{1}{RT^2} \sum_{i=1}^n x_i \sum_{j>1}^n x_j \Delta_{ij} H^2 \quad (16)$$

The contribution  $\Delta C_{\text{vib}}$  was estimated using heat capacity of the glass and the difference  $(\alpha_p(l) - \alpha_p(gl))$ . To find the hole contribution, the enthalpies of vaporization and  $(\alpha_p(l) - \alpha_p(gl))$  were

needed. We identified hole contributions greater than  $0.80 \cdot \Delta_{\text{gl}}^1 C_p$  [48]. Similar results were obtained for the heat-capacity change at fusion.

#### *4.2. Thermodynamic properties of plastic crystals of organic compounds*

Plastic crystals can be defined as molecular crystalline phases in which there is a possibility of molecular rotation without changes of the positions of the centers of mass of the molecules (figure 13). These rotations are reflected in their thermodynamic, mechanical, dielectric, and spectral properties [75, 76].

Our studies of phase transitions of cyclic alcohols, halogen-substituted cycloalkanes, cage hydrocarbons, and adamantanes made it possible to establish the following trends [54, 77, 78, 79, 80, 81, 82, 83, 84, 85]:

1. It is impossible to predict the ability of substances to form plastic crystals based solely on their molecular structure.
2. The temperature ranges of stability of the plastic crystal phase can vary from a fraction of a kelvin to  $> 100$  K (figure 14).
3. For a majority of substances that form plastic crystals,  $\Delta S \geq 2R$  for transitions into the plastic phase,  $\Delta S \leq R$  for fusion.
4. Transitions of the type rigid crystal  $\rightarrow$  plastic crystal are accompanied by a sharp increase in heat capacity (figure 15), where  $\Delta C_p$  varies from about zero to  $100 \text{ J} \cdot \text{mol}^{-1} \cdot \text{K}^{-1}$ .
5. IR-spectroscopic studies of organic compounds at various temperatures proved that, in the plastic phase, substances exist as mixtures of conformers similar to liquids. In the rigid crystal phase, all molecules in the lattice have a single conformation.

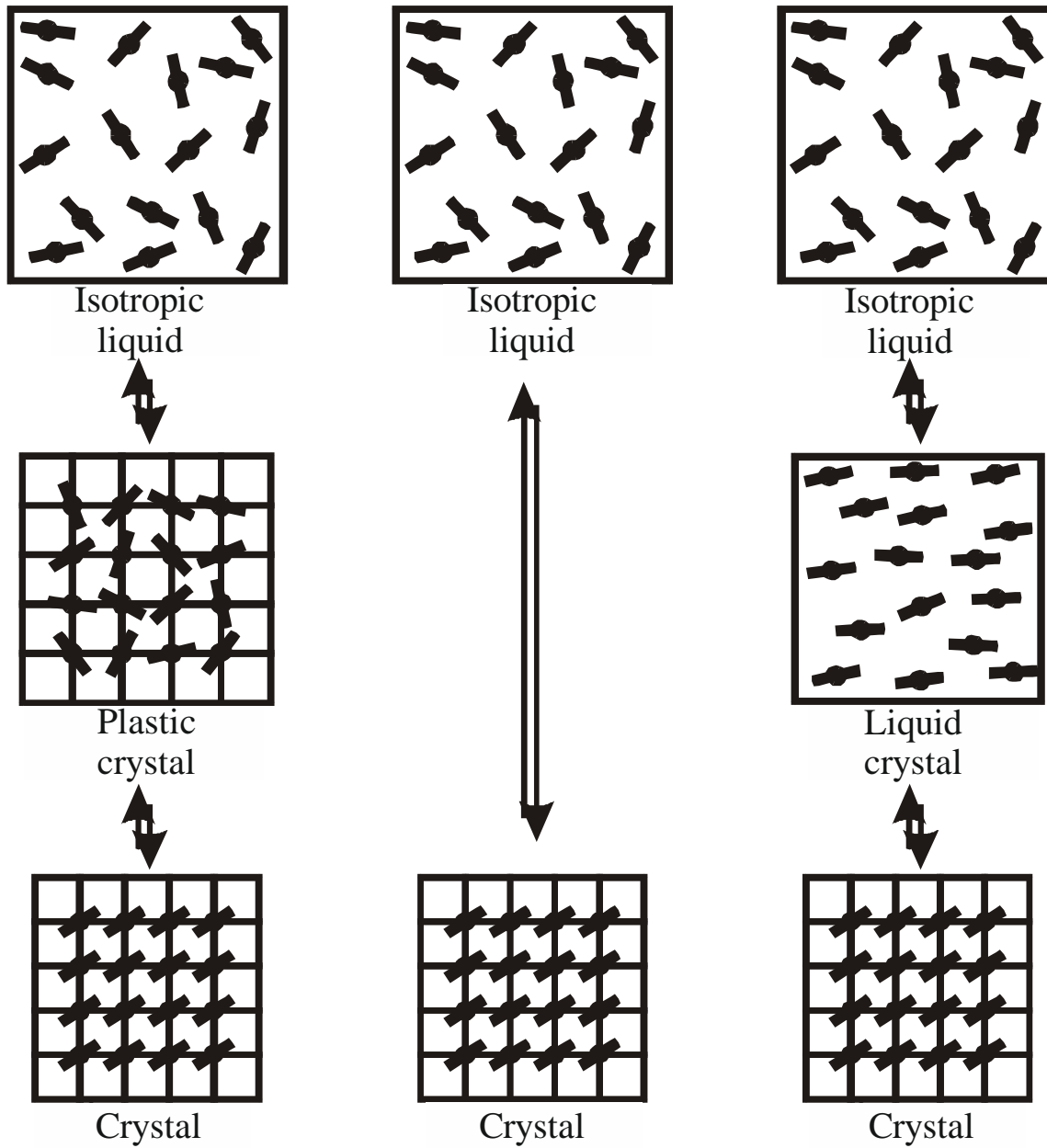


**FIGURE 13.** Possible transition pathways from rigid crystal to isotropic liquid.

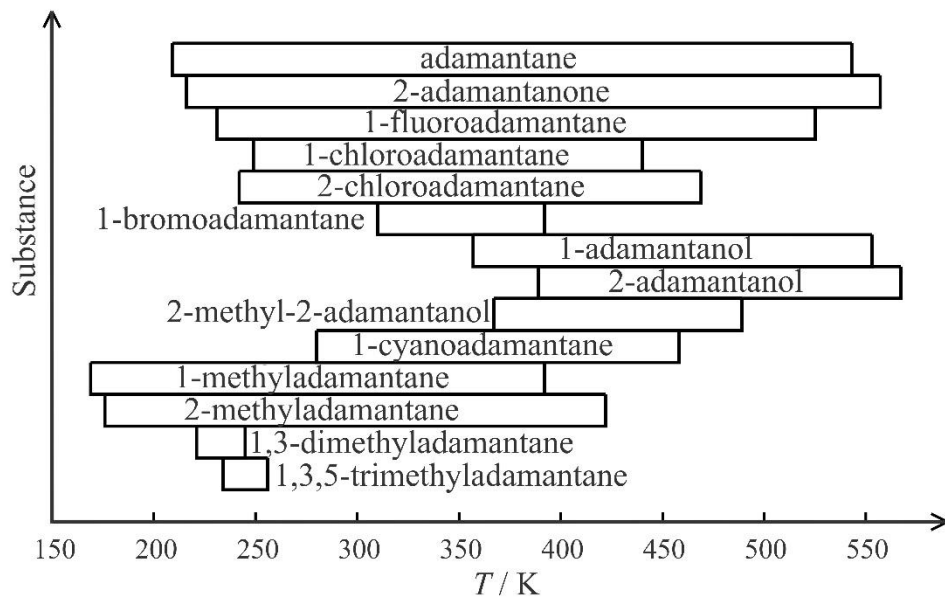


**FIGURE 14.** Temperature ranges of plastic crystal phase existence for adamantane and its derivatives. Adapted from [76].

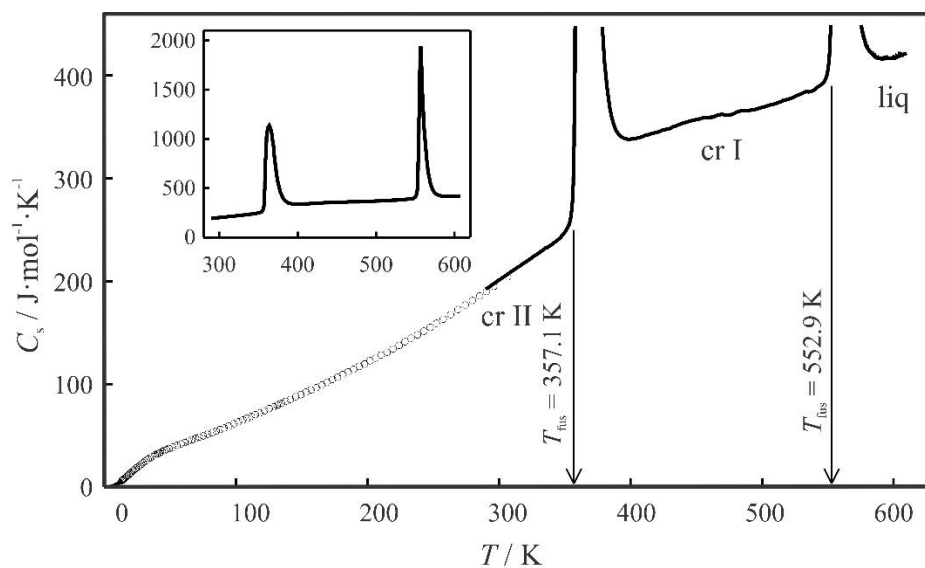


**FIGURE 15.** Temperature dependence of heat capacity of 1-adamantanol in the condensed state at the saturation line:  $\circ$ , adiabatic calorimetry; solid line, differential scanning calorimetry. Adapted from [76].

The entropy and heat capacity changes at the phase transitions from rigid crystal to plastic crystal were presented as follows:

$$\Delta_{\text{tr}}S = \Delta S_v + \Delta S_{\text{conf}} + \Delta S_{\text{or}} \quad (17)$$

$$\Delta_{\text{tr}}C_p = \Delta C_{p,v} + \Delta C_{p,\text{conf}} + \Delta C_{p,\text{or}} \quad (18)$$

where  $\Delta S_v$  and  $\Delta C_{p,v}$  were contributions caused by volume changes;  $\Delta S_{\text{conf}}$  and  $\Delta C_{p,\text{conf}}$  were conformational contributions; and  $\Delta S_{\text{or}}$  and  $\Delta C_{p,\text{or}}$  were orientational contributions. We showed [54] that  $\Delta S_v \approx 0.4\Delta_{\text{tr}}S$  and  $\Delta C_{p,v} \approx 0$ . Conformational contributions were calculated using eqs. (8) and (16). Direct experimental measurements only enable confirmation of discrete orientational changes for molecules in plastic crystals. Unfortunately, these measurements do not provide any information about the distribution of energy states resulting from non-equivalent orientations of molecules,  $n_{\text{or}}$ , nor about differences in energy,  $\Delta_{\text{or}}E$ , between them. In Ref. [86], we considered various physical models for estimation of  $\Delta S_{\text{or}}$  and  $\Delta C_{p,\text{or}}$  in plastic crystals of organic substances. These models were based on the following principles:

1. In a plastic crystal, there are a number of energetically non-equivalent rotational orientations.
2. There is a single lowest energy level.
3. The entropy of each ensemble consisting of only molecules in one of rotational orientation is postulated to be the same as all others.
4. The distribution of molecules between energy states does not depend on molecular conformations.

Our analysis consisted of finding a number of non-equivalent orientations,  $n_{\text{or}}$ , and energy differences between these orientations,  $\Delta_{\text{or}}E$ . Solutions for  $n_{\text{or}}$  and  $\Delta_{\text{or}}E$  had to be consistent with the target values of both  $\Delta S_{\text{or}}$  and  $\Delta C_{p,\text{or}}$ . In turn, the values of  $\Delta S_{\text{or}}$  and  $\Delta C_{p,\text{or}}$  were determined on the basis of experimentally measured heat capacity as well as temperature and enthalpy of

transition. These solutions were found as intersections of iso-entropic curves,  $\Delta S_{\text{or}}(n_{\text{or}}, \Delta_{\text{or}}E) = \text{const}$ , and curves of constant heat capacity,  $\Delta C_{p,\text{or}}(n_{\text{or}}, \Delta_{\text{or}}E) = \text{const}$ , plotted for the temperature of the phase transition (figure 16).

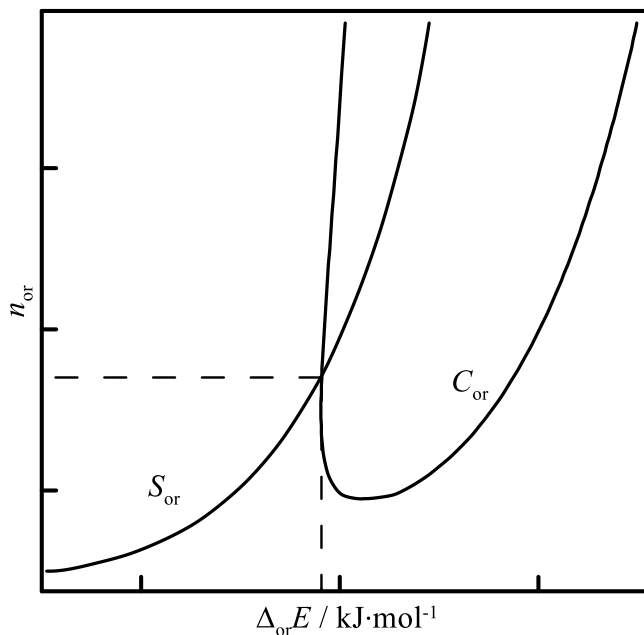


**FIGURE 16.** Typical iso-entropic  $\Delta S_{\text{or}} = \text{const}$  and iso-heat-capacity  $\Delta C_{\text{or}} = \text{const}$  curves in coordinates  $n_{\text{or}} - \Delta_{\text{or}}E$  for the “rigid crystal  $\rightarrow$  plastic crystal” phase transition. Adapted from Ref. [48] with permission from the Royal Society of Chemistry.

It was shown that the best agreement with the values of  $\Delta S_{\text{or}}$  and  $\Delta C_{p,\text{or}}$  for various plastic crystals of organic substances was reached with models of orientational energy states formulated as (figure 17),

$$\Delta_{ij}H \approx \Delta_{ij}E = \sum_{k=i}^{j-1} f(k)\Delta_{\text{or}}E \quad (19)$$

$$f_a(k) = \begin{cases} 1, & \text{if } k=1 \\ 0, & \text{if } k>1 \end{cases}, \text{ or } f_b(k) = 2^{1-k}, \text{ or } f_c(k) = k^{-1} \quad (20)$$

where  $f(k)$  was an energy distribution function for various molecular orientations.

As demonstrated for a number of plastic crystals [86], the results obtained with the use of the three models presented by eqs. (19) and (20) agreed reasonably well. The proposed methods are now the only ones available for estimation of numbers of non-equivalent orientations and their energy states in plastic crystals of organic substances.

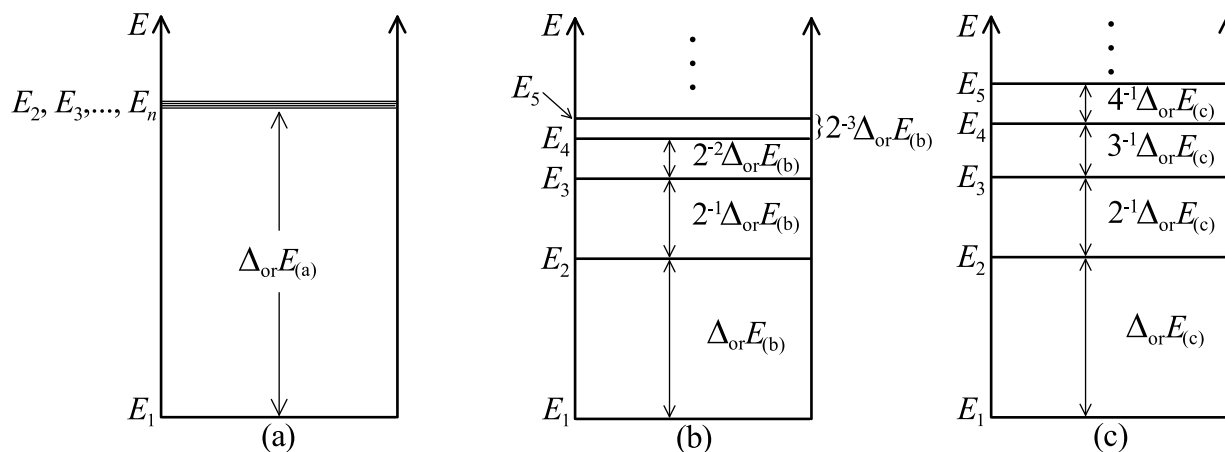


**FIGURE 17.** Various cases of energy levels distribution in a plastic crystal. Reproduced from Ref. [48] with permission from the Royal Society of Chemistry.

#### 4.3. Thermodynamic properties of ionic liquids

Room-temperature ionic liquids (ILs) are formed by bulky, often asymmetric, organic cations and organic or inorganic anions (figure 18).

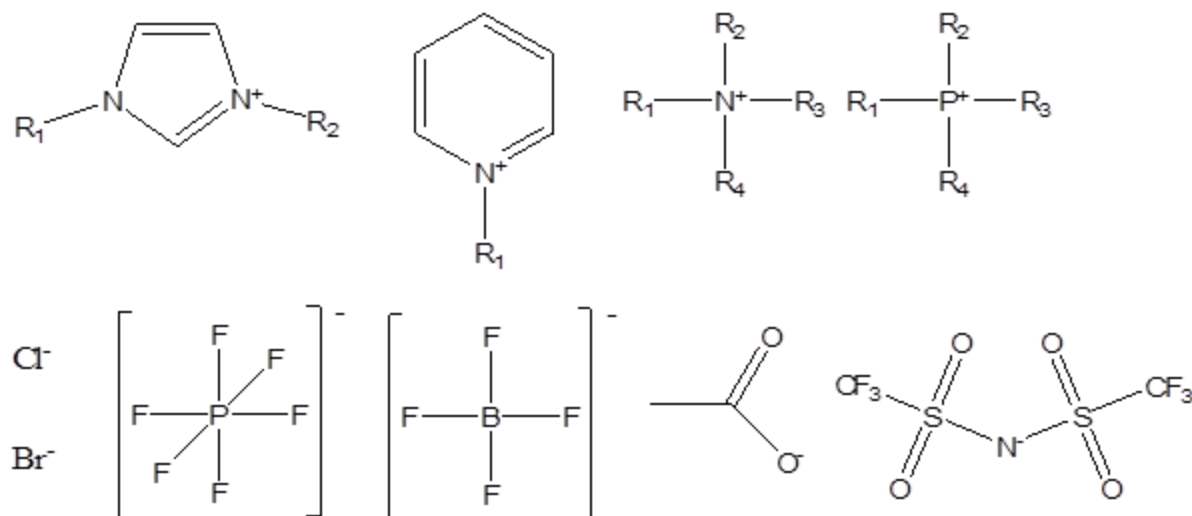


**FIGURE 18.** Typical cations and anions of ILs

A wide liquid range ( $\sim 270$  to  $500$  K), very low vapor pressure ( $p_s(298\text{ K}) < 10^{-8}$  Pa), high electrical conductivity, and capability to dissolve broad classes of materials are characteristic for these substances. ILs have demonstrated their potential in various applications and technologies: as catalytic systems, selective extracting agents, electrolytes for batteries, supercapacitors, components of electrolytic systems, heat transfer fluids, and solvents for polymers and biopolymers. To justify conditions for industrial IL synthesis and their efficient technical use, a thermodynamic analysis of the corresponding processes is required. As a result, over the last two decades, thermodynamic properties of ILs have been actively studied [87, 88].

In 2001, following the suggestion by Dr. Joseph W. Magee (NIST, USA), we started a unique program of systematically measuring the thermodynamic properties of these substances. So far, over 20 ILs have been studied by adiabatic calorimetry, which included measurements of heat capacities, temperatures and enthalpies of phase transitions, as well as parameters of glass transitions in the temperature range ( $5$  to  $370$ ) K. Most of the studied compounds are 1-alkyl-3-methylimidazolium ILs with various anions (Table 3).

Heat capacities of ILs in the liquid state available in the literature were analyzed [89] and a set of mutually consistent uncertainties for these results was obtained. Recommended heat capacities over a wide range of temperatures were derived for 23 ILs [89]. These recommendations were recently extended to a larger number of ILs [90].

The vapor pressure of ILs was first measured in our laboratory [91, 92]. Using these results, we determined thermodynamic parameters of vaporization for  $[C_n\text{mim}]\text{NTf}_2$  ILs,  $n = 2, 4, 6,$  and  $8$ . Molecular geometries, frequencies, and parameters of internal rotation necessary to calculate ideal-gas thermodynamic properties of ILs were found with the use of quantum-chemical methods. The calculated entropies agreed well with the values determined from the experimental data [70]. It was demonstrated that, in the temperature range considered, ILs exist in the form of ionic pairs in the gas phase.

Complex polymorphism was found in the  $[C_n\text{mim}]\text{NTf}_2$  family. Multiple melting points as well as solid-to-solid phase transitions were identified [97, 106, 36]. The polymorphs were studied by IR spectroscopy and X-ray diffraction at different temperatures [93]. Characteristic conformations of the cations and anions in the various phases were determined.

Based on the thermodynamic properties obtained, the following predictive procedures were developed.

**TABLE 3**ILs studied by adiabatic calorimetry in our laboratory and appropriate references <sup>a</sup>

| Cation                             | Anion           |                |                                  |                                  |                              |                                |                                 |                              |                              |                  |        |                               |
|------------------------------------|-----------------|----------------|----------------------------------|----------------------------------|------------------------------|--------------------------------|---------------------------------|------------------------------|------------------------------|------------------|--------|-------------------------------|
|                                    | Br <sup>-</sup> | I <sup>-</sup> | CH <sub>3</sub> COO <sup>-</sup> | CF <sub>3</sub> COO <sup>-</sup> | BF <sub>4</sub> <sup>-</sup> | EtSO <sub>4</sub> <sup>-</sup> | N(CN) <sub>2</sub> <sup>-</sup> | NO <sub>3</sub> <sup>-</sup> | PF <sub>6</sub> <sup>-</sup> | Tos <sup>-</sup> | OTf    | NTf <sub>2</sub> <sup>-</sup> |
| [C <sub>2</sub> mim] <sup>+</sup>  | 94              |                |                                  |                                  |                              | 95,96                          |                                 |                              |                              |                  |        | 97 <sup>c</sup>               |
| [C <sub>3</sub> mim] <sup>+</sup>  | 94,96,<br>98    |                |                                  |                                  |                              |                                |                                 |                              |                              |                  |        |                               |
| [C <sub>4</sub> mim] <sup>+</sup>  | 94              | 98             | 99                               | 99                               | 95,96                        |                                | 96 <sup>b</sup>                 | 100                          | 69,<br>101,102               | 103              | 104,96 | 105                           |
| [C <sub>6</sub> mim] <sup>+</sup>  |                 |                |                                  |                                  |                              |                                |                                 |                              |                              |                  |        | 36 <sup>c</sup>               |
| [C <sub>8</sub> mim] <sup>+</sup>  |                 |                |                                  |                                  | 95,96                        |                                |                                 |                              |                              |                  |        | 97                            |
| [C <sub>10</sub> mim] <sup>+</sup> |                 |                |                                  |                                  |                              |                                |                                 |                              |                              |                  |        | 106                           |
| [C <sub>14</sub> mim] <sup>+</sup> |                 |                |                                  |                                  |                              |                                |                                 |                              |                              |                  |        | 96,106                        |
| [C <sub>16</sub> mim] <sup>+</sup> |                 |                |                                  |                                  |                              |                                |                                 |                              |                              |                  |        | 106                           |
| [BuMe <sub>3</sub> N] <sup>+</sup> |                 |                |                                  |                                  |                              |                                |                                 |                              |                              |                  |        | 96 <sup>b</sup>               |
| [C <sub>4</sub> mPr] <sup>+</sup>  |                 |                |                                  |                                  |                              |                                |                                 |                              |                              |                  |        | 96 <sup>b</sup>               |

<sup>a</sup> [C<sub>n</sub>mim]<sup>+</sup>, 1-alkyl-3-methylimidazolium; [BuMe<sub>3</sub>N]<sup>+</sup>, butyltrimethylammonium; [C<sub>4</sub>mPr], 1-butyl-1-methylpyrrolidinium; EtSO<sub>4</sub><sup>-</sup>, ethyl sulfate; Tos<sup>-</sup>, *p*-methylbenzenesulfonate; OTf, trifluoromethanesulfonate; NTf<sub>2</sub><sup>-</sup>, bis(trifluoromethanesulfonyl)imide;

<sup>b</sup> only liquid-phase heat capacities and melting parameters were reported

<sup>c</sup> heat capacity of [C<sub>2</sub>mim]NTf<sub>2</sub> + [C<sub>6</sub>mim]NTf<sub>2</sub> is reported in Ref. [107]

1. Heat capacity per unit volume ( $C_p/V$ ) was  $1.95 \text{ J}\cdot\text{K}^{-1}\cdot\text{cm}^{-3}$  for many ILs at  $T = 298.15 \text{ K}$  and  $p = 0.1 \text{ MPa}$  [95], and the deviations did not exceed  $\pm 10 \%$  of this value for the set considered. This quotient weakly changed with temperature:

$$(C_p/V) / (\text{J}\cdot\text{K}^{-1}\cdot\text{cm}^{-3}) = 1.951 + 8.33 \cdot 10^{-4} \cdot ((T / \text{K}) - 298.15) \quad (21)$$

The liquid-phase heat capacities of ILs in the range from  $T_g$  to  $370 \text{ K}$  were correlated with the vibrational and conformational contributions of the ions [99, 108]. Deviations of the calculated values were within  $\pm 0.03 C_p$  of their experimental counterparts [108].

2. Additivity of IL heat capacities was demonstrated [89]. A substitution scheme based on the anion increments  $\Delta C_p(\text{NTf}_2 \rightarrow \text{X})$  was proposed. The temperature-dependent increments were described with the equation:

$$\Delta C_p(\text{NTf}_2 \rightarrow \text{X}) / (\text{J}\cdot\text{K}^{-1}\cdot\text{mol}^{-1}) = b_1 + 10^{-2}c_1(T / \text{K}) + 10^{-4}d_1(T / \text{K})^2, \quad (22)$$

whose coefficients are listed in Table 4 [109].

**TABLE 4**

Coefficients of Eq. (22)

| X                               | $b_1$  | $c_1$   | $d_1$   | $T$ range / K |
|---------------------------------|--------|---------|---------|---------------|
| Br                              | -189.0 | -26.913 | 1.5539  | 230 to 370    |
| BF <sub>4</sub>                 | -170.0 | -3.431  | -1.4332 | 250 to 370    |
| CF <sub>3</sub> SO <sub>3</sub> | -49.2  | -27.871 | 1.5539  | 315 to 425    |
| EtSO <sub>4</sub>               | 304.5  | -81.118 | 13.762  | 200 to 370    |
| PF <sub>6</sub>                 | -157.8 | -4.945  | 1.5539  | 200 to 330    |
| CH <sub>3</sub> COO             | -62.9  | -76.776 | 12.172  | 210 to 370    |
| CF <sub>3</sub> CO <sub>2</sub> | -117.0 | -18.736 | 1.5539  | 190 to 370    |

|                 |        |         |        |            |
|-----------------|--------|---------|--------|------------|
| Tos             | -73.5  | 1.909   | 1.5539 | 350 to 370 |
| NO <sub>3</sub> | -145.6 | -27.324 | 1.5539 | 310 to 370 |

An incremental scheme using the equation

$$C_p([\text{C}_n\text{Cat}]\text{An}) = C_p([\text{C}_6\text{mim}]\text{NTf}_2) + (n - 6)\Delta C_p(\text{H} \rightarrow \text{CH}_3) + \Delta C_p(\text{NTf}_2 \rightarrow \text{An}) + \Delta C_p([\text{C}_6\text{mim}] \rightarrow [\text{C}_6\text{Cat}]) \quad (23)$$

was developed [108]. A similar approach was proposed for the IL entropy in the liquid phase.

3. The solid-phase enthalpies of formation  $\Delta_f H^\circ$  of potassium salts at  $T = 298.15$  K were correlated with  $\Delta_f H^\circ$  of imidazolium ILs [110] using the equations:

$$\Delta_f H^\circ([\text{C}_4\text{mim}]\text{An}) = \Delta_f H^\circ([\text{C}_4\text{mim}]\text{Br}) + \Delta\Delta_f H^\circ(\text{KBr} \rightarrow \text{KAn}) \quad (24)$$

$$\Delta_f H^\circ([\text{C}_4\text{mim}]\text{An}) = \Delta_f H^\circ([\text{C}_4\text{mim}]\text{NO}_3) + \Delta\Delta_f H^\circ(\text{KNO}_3 \rightarrow \text{KAn}). \quad (25)$$

The increments were estimated for the anions NO<sub>3</sub><sup>-</sup>, F<sup>-</sup>, Cl<sup>-</sup>, MnO<sub>4</sub><sup>-</sup>, HS<sup>-</sup>, CNO<sup>-</sup>, CN<sup>-</sup>, ClO<sub>4</sub><sup>-</sup>, ClO<sub>3</sub><sup>-</sup>, and BF<sub>4</sub><sup>-</sup>.

4. The enthalpies of vaporization  $\Delta_{\text{vap}} H^\circ$  for ILs known for their low vapor pressure can hardly be directly measured in calorimeters working at  $T < 550$  K. Therefore, development of empirical predictive procedures is of high priority. Initially, we proposed a correlation based on the Stefan equation [92], which predicted  $\Delta_{\text{vap}} H^\circ$  at  $T = 298.15$  K based on the surface tension  $\sigma$  and molar volume  $V_m$ :

$$\Delta_{\text{vap}} H^\circ = A(\sigma V_m^{2/3} \cdot N_A^{1/3}) + B, \quad (26)$$

where  $N_A$  is the Avogadro's number and  $A$  and  $B$  are the empirical coefficients.

Several empirical correlations based on the molar mass,  $M$ , molar volume,  $V_m$ , or density,  $\rho$ , and surface tension,  $\sigma$ ,

$$\Delta_{\text{vap}} H^\circ = f(M, V_m(\text{or } \rho), \sigma) \quad (27)$$

were obtained with symbolic regression approaches [111]. These correlations describe the experimental enthalpies of vaporization for 19 ILs at  $T = 450$  K quite well. For example, a four-parameter correlation described the experimental data within  $\pm 6$   $\text{kJ}\cdot\text{mol}^{-1}$ . Additionally, a procedure for estimation of  $\Delta_{\text{vap}}H^\circ$  at  $T = 450$  K using the increments for substitution of the cation base as well as substituents and the anions in the reference substance  $[\text{C}_1\text{mim}]\text{NTf}_2$  was developed [111].

#### *4.4. Thermodynamic properties of carbon allotropes: fullerenes $\text{C}_{60}$ and $\text{C}_{70}$ and multi-walled carbon nanotubes*

It is well-known that carbon allotropes (graphite, diamond, fullerenes, and nanotubes) have distinct physical properties and have a range of uses in technical materials and devices. To better understand conditions for the synthesis and use of fullerenes, their hydrides, and carbon nanotubes, we carried out thermodynamic studies and expert evaluation of the available thermodynamic and structural data.

Based on detailed analysis of multiple experimental studies of the thermodynamic properties of fullerenes  $\text{C}_{60}$  and  $\text{C}_{70}$ , recommended values for  $C_p(T)$ ,  $\Delta_{\text{sub}}H(T)$ , and  $p_s$  were derived. The most reliable spectroscopic results were selected for statistical thermodynamics calculations for  $\text{C}_{60}$  and  $\text{C}_{70}$ . The suggested set of frequencies of intramolecular vibrations provided good agreement with the experimental and calculated heat capacities of crystalline  $\text{C}_{60}$  and  $\text{C}_{70}$  in the temperature range (300 to 550) K [112]. Analysis of heat capacity data let us conclude that the hindered rotation of  $\text{C}_{60}$  molecules occurs above the solid-to-solid phase transition at  $T_{\text{tr}} = 260.7$  K [113]. The effective potential barrier was estimated to be  $5$   $\text{kJ}\cdot\text{mol}^{-1}$ . A similar barrier for crystalline  $\text{C}_{70}$  was about  $3$   $\text{kJ}\cdot\text{mol}^{-1}$ . Unlike most organic compounds, crystalline  $\text{C}_{60}$  and  $\text{C}_{70}$  have two inflection points in

their heat capacity curves. This behavior results from the low Debye temperatures equal to 46 K and 40 K, respectively, and low frequencies of librations. Ideal-gas thermodynamic properties for fullerenes were calculated in the temperature range (100 to 5000) K using statistical thermodynamics. The resulting entropies,  $S^\circ(\text{C}_{60}, 860 \text{ K}) = 1464 \text{ J}\cdot\text{K}^{-1}\cdot\text{mol}^{-1}$  and  $S^\circ(\text{C}_{70}, 843.5 \text{ K}) = 1669 \text{ J}\cdot\text{K}^{-1}\cdot\text{mol}^{-1}$ , deviated from the experimental values by (1.0 to 1.5) %, which did not exceed the experimental uncertainties.

Heat capacities of the stacked-cup multi-walled carbon nanotubes (MWCNT) were measured in an adiabatic calorimeter in the range (5 to 370) K. The energy of combustion  $\Delta_c u^\circ(298.15 \text{ K}) = -(32809 \pm 73) \text{ J}\cdot\text{g}^{-1}$  for the carbon-only material was found by correcting the experimental value determined in an isoperibol combustion calorimeter for elemental composition of the dried sample. The solid residue after the combustion experiments corresponded to NiO oxide formed from a  $6.9\cdot 10^{-3}$  mass fraction of nickel. This metal could not be removed from the material by magnetic separation [114].

The apparent density of MWCNT [115],  $\rho = (2.21 \pm 0.02) \text{ g}\cdot\text{cm}^{-3}$  at  $T = 293 \text{ K}$ , was found from experimental densities of the suspensions with water, toluene, and [C<sub>4</sub>mim]PF<sub>6</sub>. Densities for the IL-containing systems could be determined for both the liquid-filled and hollow MWCNT. These results made it possible to estimate geometrical characteristics of the material.

The heat capacity of MWCNT exceeded that of graphite by  $(3.3 \text{ to } 3.6)\cdot 10^{-2} c_p$  in the temperature range (300 to 370) K [114]. This similarity was used to estimate thermodynamic properties of MWCNT at  $T > 370 \text{ K}$ . The enthalpies of formation, heat capacities, and entropies of MWCNT are close to those of graphite above  $T = 200 \text{ K}$  (Table 5). This is physically justified since the distances between the carbon layers in MWCNT ( $\approx 0.36 \text{ nm}$ ) and in graphite (0.3355 nm [116]) are close and the density of MWCNT is comparable with that of graphite ( $\rho = 2.265 \text{ g}\cdot\text{cm}^{-3}$  [116]).

Crystalline fullerenes are less stable than graphite due to the higher enthalpies of formation. It was demonstrated [117] that the thermodynamic instability of crystalline C<sub>60</sub> and C<sub>70</sub> relative to graphite holds to a temperature of 3000 K and a pressure of 20 GPa. However, in the gas phase, the equilibrium radically shifts towards the fullerenes due to significantly lower enthalpies of sublimation for C<sub>60</sub> and C<sub>70</sub>. Thus, the successful synthesis of the fullerenes was realized through high-temperature sublimation of carbon [118].

**TABLE 5**

Thermodynamic properties of different forms of carbon <sup>a,b</sup>

| Carbon form                    | $T / \text{K}$ | $\Delta_f H^\circ(T) /$<br>$\text{kJ}\cdot\text{mol}^{-1}$ | $C_p^\circ(T) /$<br>$\text{J}\cdot\text{K}^{-1}\cdot\text{mol}^{-1}$ | $S^\circ(T)-S^\circ(0) /$<br>$\text{J}\cdot\text{K}^{-1}\cdot\text{mol}^{-1}$ | $\Delta_f G^\circ(T) /$<br>$\text{kJ}\cdot\text{mol}^{-1}$ |
|--------------------------------|----------------|--|--|---|--|
| Graphite                       | 298.15         | 0  | $8.517 \pm 0.009$  | $5.74 \pm 0.10$   | 0  |
| [119,120]                      | 1000           | 0  | $21.610 \pm 0.022$   | $24.46 \pm 0.10$  | 0  |
| MWCNT [114]                    | 298.15         | $0.6 \pm 0.9$  | $8.842 \pm 0.035$  | $6.225 \pm 0.025$   | $0.5 \pm 0.9$  |
|                                | 1000           | $1.0 \pm 0.9$  | 22.3   | 25.5  | $-(0.1 \pm 0.9)$   |
| Fullerene C <sub>60</sub> (cr) | 298.15         | $39.1 \pm 0.2$   | $8.760 \pm 0.044$  | $7.118 \pm 0.036$   | $38.7 \pm 0.2$   |
| [112]                          | 1000           | $37.6 \pm 0.2$   | $21.35 \pm 0.21$   | $25.87 \pm 0.26$  | $36.2 \pm 0.4$   |
| Fullerene C <sub>70</sub> (cr) | 298.15         | $36.5 \pm 0.3$   | $8.937 \pm 0.045$  | $6.467 \pm 0.032$   | $36.3 \pm 0.3$   |
| [112]                          | 1000           | $36.6 \pm 0.3$   | $21.46 \pm 0.21$   | $25.41 \pm 0.25$  | $35.6 \pm 0.4$   |

<sup>a</sup> expanded uncertainties for 0.95 confidence interval are given in the table

<sup>b</sup> per mole of carbon atoms

## 5. Thermodynamic properties of substances and technological applications

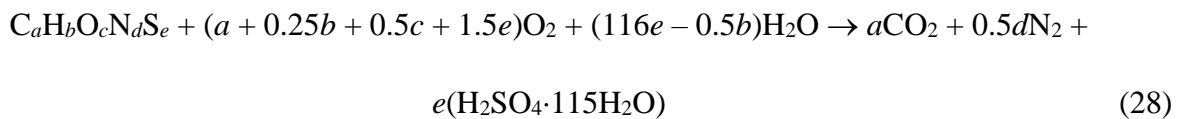
### 5.1. Chemical exergy of organic substances and a thermochemical model of the environment

Exergy of a system  $E = H - T_0S$  is defined as the maximum work performed in a reversible process of devaluation with the environment. Exergy is a universal indicator of the thermodynamic value of raw materials and the degree of thermodynamic perfection of technological processes. The part of exergy associated with chemical transformations is called chemical exergy  $E_{ch}$ . For calculation of chemical exergies, parameters of the environment are of crucial significance. Since the real environment is a non-equilibrium system, a commonly accepted set of its parameters does not exist.

#### 5.1.1. Thermochemical model of the reference environment

The thermochemical model of the environment we developed [121, 122] was based on the following principles:

1. The final products of element transformations in combustion calorimetry were selected as the reference substances:



2. Concentrations of the gaseous reference substances  $N_2$ ,  $O_2$ ,  $CO_2$  were assumed to be equal to their atmospheric concentrations at a humidity of 100 %.

3. The concentration components of exergy for solid reference substances and liquid water were taken equal to zero.

4. The devaluation reaction was an ideal reaction of combustion in a calorimetric bomb. The auxiliary materials and by-products were not considered.

5. The reference temperature and pressure were  $T_0 = 298.15$  K,  $p_0 = 101.3$  kPa, respectively.

A devaluation diagram for  $C_aH_bO_cN_dS_e$ -type substances is presented in figure 19.

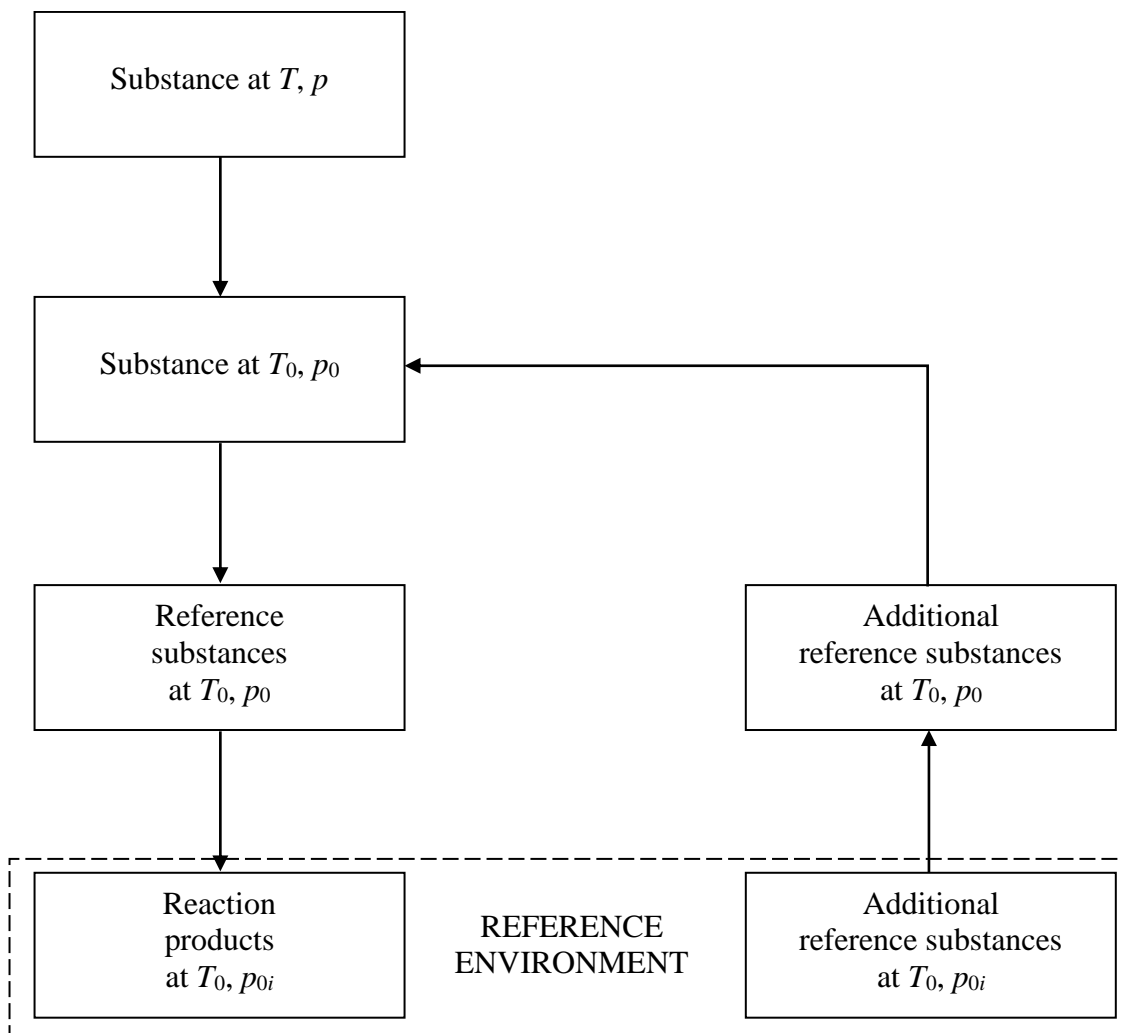


**FIGURE 19.** Scheme of the substance devaluation process, where  $T$  and  $p$  are the temperature and pressure of a substance;  $T_0$  and  $p_0$  are the reference temperature and pressure;  $p_{0i}$  is the partial pressure of the  $i$ th reference substance in the environment

Prof. Alexander A. Kozyro created a database of chemical exergies for the main products, intermediates, and by-products of chemical industry of the Republic of Belarus, including

production of ammonia, nitric and sulfuric acids,  $\varepsilon$ -caprolactam, hydroxyammonium sulfate, urea, and dimethyl terephthalate. This database contains about 500 numerical values of standard enthalpies,  $\Delta_{\text{dev}}H^\circ$ , entropies,  $\Delta_{\text{dev}}S^\circ$ , Gibbs energies,  $\Delta_{\text{dev}}G^\circ$ , of devaluation reactions and chemical exergies,  $E^\circ_{\text{ch}}$ , calculated mainly from the values of thermodynamic properties determined in the Laboratory of Thermodynamics of Organic Compounds of the Belarusian State University.

### *5.1.2. Additivity of chemical exergies*

Property predictions using a group-contribution approach are of significant practical importance. They make it possible to estimate exergies, avoiding expensive calorimetric measurements of combustion energies, heat capacities, and enthalpies of phase transitions as well as determination of vapor pressures. It was demonstrated [122, 123] that chemical exergies could be accurately predicted using group-contribution methods though the exergies included  $\Delta_{\text{dev}}H^\circ$  and  $\Delta_{\text{dev}}S^\circ$ , which are non-additive by physical nature. We justified the use of group-contribution methods in this case and determined numerical values of the temperature-dependent increments for large-scale calculations of chemical exergies for liquid and gaseous alkanes, alkenes, alkyl substituted benzenes, cyclohexanes, and cyclopentanes in the range  $T = (298 \text{ to } 1000) \text{ K}$ .

### *5.1.3. Chemical exergy of mixtures and fuels*

Chemical exergy of mixtures and fuels can be calculated, if the detailed composition and thermodynamic properties of all components are known. This is often unattainable, thus, alternative methods for determining exergy of materials are needed. We demonstrated [124] that chemical exergies could be estimated with the use of experimental thermodynamic properties of the material,  $\Delta_c H^\circ(T)$  and  $S^\circ(T) - S^\circ(0)$ . A ten-component model mixture of hydrocarbons of

composition  $C_{7.367}H_{14.124}$  was prepared. The differences between exergies found from the properties of individual components and from experimental data for the mixture were 0.07 % at  $T = 298.15$  K.

The enthalpy of combustion  $\Delta_c H^\circ$  is a principal property of interest for fuels, and relatively easily determined. It was shown that the contributions to chemical exergy due to non-ideality and entropy of mixing were significantly smaller than  $\Delta_c H^\circ$  itself. Therefore, it was reasonable to use correlation equations of a general type  $E_{ch} = f(\Delta_c H^\circ)$  to predict chemical exergies for fuels. Using the thermodynamic data values for 1179 individual liquids of a general formula  $C_a H_b O_c N_d S_e$ , we obtained the correlation:

$$E_{ch} = -\Delta_c H (1.02034 - 0.01381(b'/a') + 0.03374(c'/a') + 0.02593(d'/a') + 0.08408(e'/a')) \quad (29)$$

This estimates chemical exergy for a fuel with the overall composition  $C_a H_b O_c N_d S_e$ . For the model mixture, the predicted value deviated by 0.2 % from the experimental one.

## *5.2. Thermodynamic justification of energy- and resource-saving technologies in $\epsilon$ -caprolactam and urea production [64, 125, 126, 127, 128, 129, 130, 131, 132]*

A detailed evaluation of the process flows for  $\epsilon$ -caprolactam and urea production at the Grodno Azot company (Belarus) was performed. We determined the locations of the maximum exergy loss and proposed measures for improvement of the technologies. At Grodno Azot,  $\epsilon$ -caprolactam is produced as illustrated in figure 20.

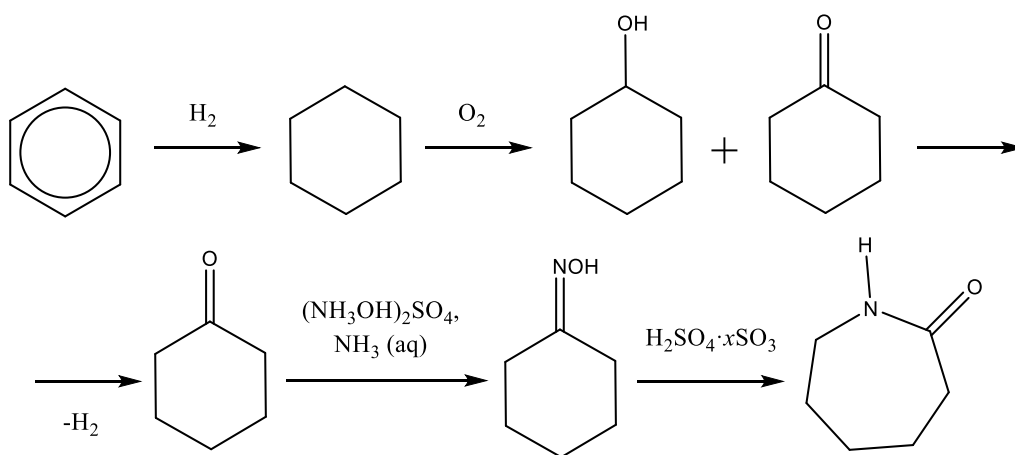
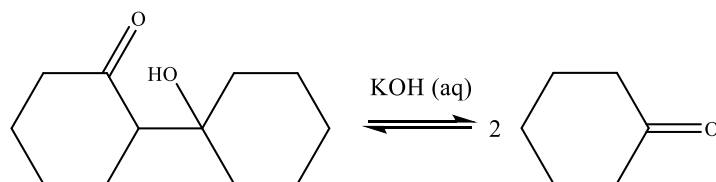


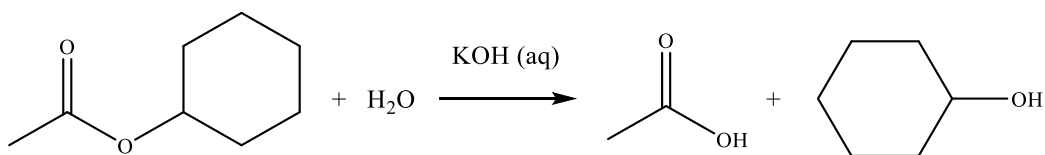
**FIGURE 20.** Scheme of  $\epsilon$ -caprolactam production

A mathematical model considering both thermodynamics and kinetics of the reaction as well as heat transfer was developed for a shell-and-tube reactor used at the benzene hydrogenation stage. Using this model, a tube filling with catalyst and inert material was proposed, which provided the optimal temperature field with no maximum inside the tubes. The implementation of this fill significantly increased duration of a turnaround interval for the hydrogenation reactor while keeping the conversion high and selective.

The by-products formed at the oxidation stage can potentially be processed to recycle cyclohexanone and cyclohexanol. Thermodynamic characteristics of decondensation of 2-(1'-hydroxycyclohexyl)cyclohexanone [133]



as well as thermodynamics and kinetics of hydrolysis of cyclohexyl acetate [134]



were studied. The optimal conditions for conversion of the oxygenated waste containing these products into the target products, cyclohexanone and cyclohexanol, were determined.

Based on the exergy analysis and mathematical modeling of the cyclohexanol dehydrogenation stage, we proposed to change the heat exchange regime in the shell-and-tube reactor from concurrent to countercurrent flow (figure 21). This improvement resulted in the increased temperature and equilibrium yield of cyclohexanone and the decreased energy consumption at the rectification stage.

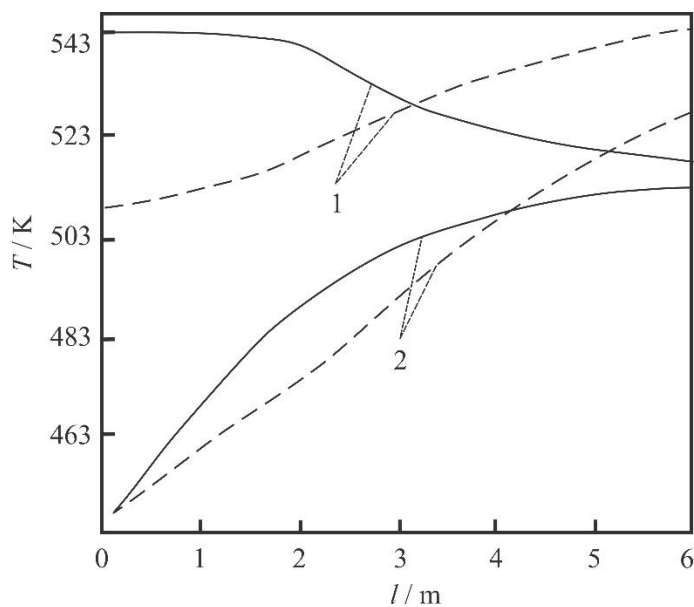


**FIGURE 21.** Temperature profiles of the dehydrogenation reactor ( $l$  is a reactor length): 1, heating gas; 2, reaction mixture; —, concurrent; ---, countercurrent [127].

Component activities in (cyclohexanone oxime (CHO) + water) were experimentally determined [127]. Based on these results, a dehydration regime at reduced pressure was proposed, which reduced the residual wetness of CHO from  $w(\text{H}_2\text{O}) = 0.05$  to 0.005. This improvement made it possible to decrease the consumption of oleum at the CHO isomerization step by ~25 %.

We studied the possibility of cyclohexanone oxime isomerization into  $\epsilon$ -caprolactam if oleum is replaced with acetic acid and if the isomerization is conducted in an IL solvent. Also, we considered various ways of product extraction from the reaction mixture. All these studies could potentially decrease irreversible consumption of oleum and ammonia used for its neutralization.

The solubility of cyclohexanone oxime and  $\epsilon$ -caprolactam in 1-alkyl-3-methylimidazolium ILs was determined [103, 135, 136]. It was found that the low solubility of cyclohexanone oxime does not permit Beckmann rearrangement in these solvents. At the same time, the  $\epsilon$ -caprolactam solubility in the protic IL  $\epsilon$ -caprolactamium trifluoroacetate was high enough to carry out this reaction. In our experiments with  $\epsilon$ -caprolactamium trifluoroacetate +  $\text{CF}_3\text{COOH}$  as a solvent and  $\text{P}_2\text{O}_5$  as a catalyst, a degree of the cyclohexanone oxime  $\rightarrow$   $\epsilon$ -caprolactam conversion near 90 % was reached even at 300 K. It seems reasonable to look for potential catalysts for industrial implementation of this process.

At Grodno Azot, urea is synthesized from  $\text{CO}_2$  and  $\text{NH}_3$ . Analysis of its production [137, 138] demonstrated that the largest exergy losses occur at the following three units:  $\text{CO}_2$  purification from sulfur-containing and combustible gases, urea synthesis, and removal of unreacted  $\text{NH}_3$  and  $\text{CO}_2$  from the urea melt. It was found that the losses of exergy can be decreased subject to the following changes in the technology:

(i) The energy of impurity combustion is used to heat  $\text{CO}_2$ .

(ii) Two reactors are used for the urea synthesis. “Fresh” CO<sub>2</sub> and NH<sub>3</sub> are supplied to the first one. The solution of ammonium carbonates and additional NH<sub>3</sub> enter the second reactor.

(iii) At the ammonia removal unit, the working pressure should be decreased from ~1.7 MPa to ~1 MPa. This will result in the temperature decrease and lower amount of the biuret by-product.

### 5.3. Thermodynamics and kinetics of ionic liquid synthesis [108, 139, 140, 141]

Heat capacities and enthalpies of phase transitions were measured in an adiabatic calorimeter for key compounds used in IL synthesis: 1-methylimidazole (mim), 1-bromobutane (BuBr), [C<sub>n</sub>mim]Br, and [C<sub>4</sub>mim]I. The entropy changes for the IL synthesis reactions were calculated. An isoperibol reaction calorimeter designed and built in our laboratory was used to determine the enthalpies of quaternization reactions in the liquid phase:



where R = ethyl, butyl, and hexyl, and Hal = Br, I. The enthalpies of reaction were in the range - (92 to 104) kJ·mol<sup>-1</sup> at T = 298.15 K. Kinetics of reaction (30) with various bromo- and iodoalkanes were studied in cyclopentanone and acetonitrile media. The Scatchard-Hildebrand equation and COSMO-SAC model were found to quantitatively describe the experimental kinetic curves over a wide range of concentrations. With the use of these thermodynamic and kinetic results, a process scheme for IL synthesis including sequential perfect-mixing and plug-flow reactors was developed. Optimal volumes of the reactors and heat-transfer surfaces, and the required flow of cooling water were evaluated for a production unit yielding 100 kg of IL per day.

#### 5.4. Thermodynamic parameters of MWCNT synthesis [114]

MWCNT are more thermodynamically stable than the crystalline fullerenes  $C_{60}$  and  $C_{70}$ . Therefore, their synthesis is possible at  $T < 1000$  K from carbon-containing precursors. However, the similarity in thermodynamic stability between graphite and MWCNT requires the use of a catalyst to increase the yield of nanotubes. The main products of propane pyrolysis at  $P = 0.1$  MPa were found to be graphite and/or MWCNT (figure 22) accompanied by gaseous  $H_2$  at  $T = 1200$  K or, at lower temperatures, methane. The relative amounts of various solid products in a real process will depend on kinetic factors, which are largely determined by the catalyst selection.

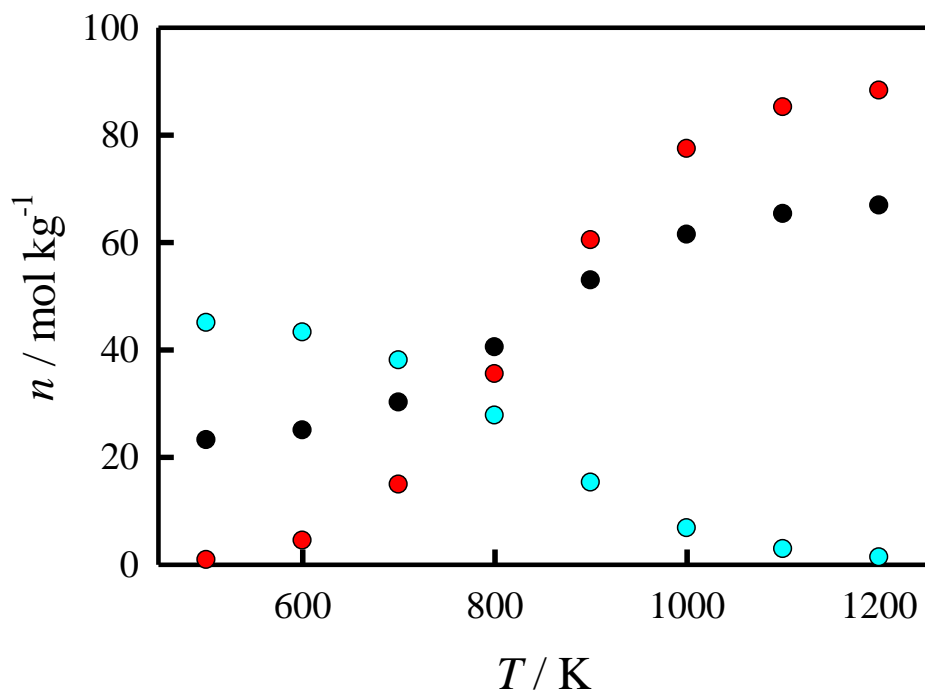


**FIGURE 22.** Calculated equilibrium composition of the pyrolysis products of propane at a pressure of 0.1 MPa: black circles, MWCNT; red circles,  $H_2$ ; cyan circles,  $CH_4$ . Adapted with permission from Ref. [114]. © 2016 American Chemical Society.

The equilibrium of the carbon monoxide disproportionation reaction



is shifted to the right-hand side below  $T = 900$  K. This reaction is exothermic, and the enthalpy factor defines its direction at low temperatures despite a significant decrease in entropy. A high yield of MWCNT in this reaction is possible at relatively low temperatures and the reaction is limited only by kinetic constraints.

#### *5.5. Thermodynamics of fullerene hydrogenation, $\text{C}_{60} + n\text{H}_2 = \text{C}_{60}\text{H}_{2n}$ [142, 143, 144]*

The thermodynamic parameters of the reactions of hydrogenation of crystalline and gaseous fullerene  $\text{C}_{60}$  to form crystalline and gaseous  $\text{C}_{60}\text{H}_2$ ,  $\text{C}_{60}\text{H}_{18}$ ,  $\text{C}_{60}\text{H}_{36}$ , and  $\text{C}_{60}\text{H}_{60}$  were determined and analyzed. A typical plot demonstrating temperature dependence of the partial equilibrium pressure of hydrogen  $p_{\text{eq}}(\text{H}_2)$  for the heterophase reaction is presented in figure 23. Equilibrium mole fractions of hydrogenated fullerenes  $x(\text{C}_{60}\text{H}_{2n})$  at various total pressures and temperatures for the gas-phase reaction are given in figure 24.

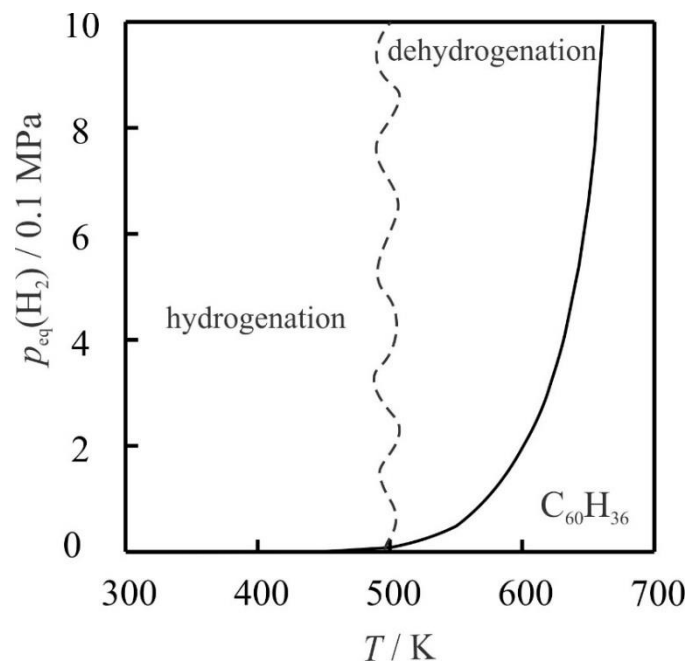


**FIGURE 23.** Decomposition pressures of  $C_{60}H_{36}$  in the crystalline state. Adapted by permission from Springer [52], © 2010.

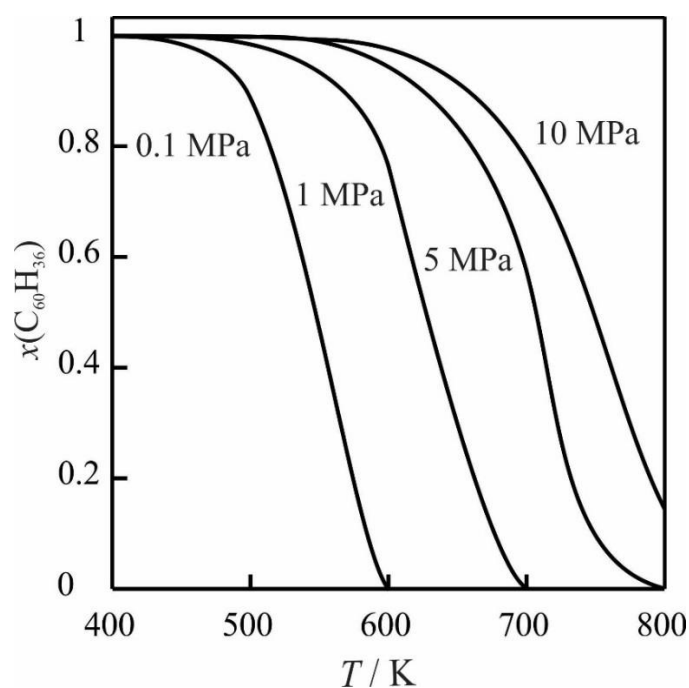


**FIGURE 24.** Dependence of equilibrium mole fraction of  $C_{60}H_{36}$  ( $x$ ) on total pressure and temperature in the reaction of gas-phase decomposition. Adapted by permission from Springer [52], © 2010.

The crystalline hydrogenated fullerenes  $C_{60}H_2$  and  $C_{60}H_{36}$  were found to be thermodynamically stable at  $T < 500$  K and  $C_{60}H_{18}$  at  $T < 650$  K. This finding can be used to improve the yield of the target hydride under the synthesis conditions. It was theoretically concluded that the experimental synthesis of perhydrofullerene  $C_{60}H_{60}$  was hardly possible because of thermodynamic limitations. The potential of the system



for use as a hydrogen accumulator was identified.

The gas-phase synthesis of  $C_{60}H_{36}$  by hydrogenation of  $C_{60}$  with 9,10-dihydroanthracene (DHA) was thermodynamically analyzed (figure 25). Since the real process is conducted in the melt, the gas-phase equilibrium constants would be close to the experimental ones. It was found that the 4-fold excess of DHA, which is less than that applied in the preparative synthesis by a factor of (1.5 to 2) provides almost quantitative hydrogenation.

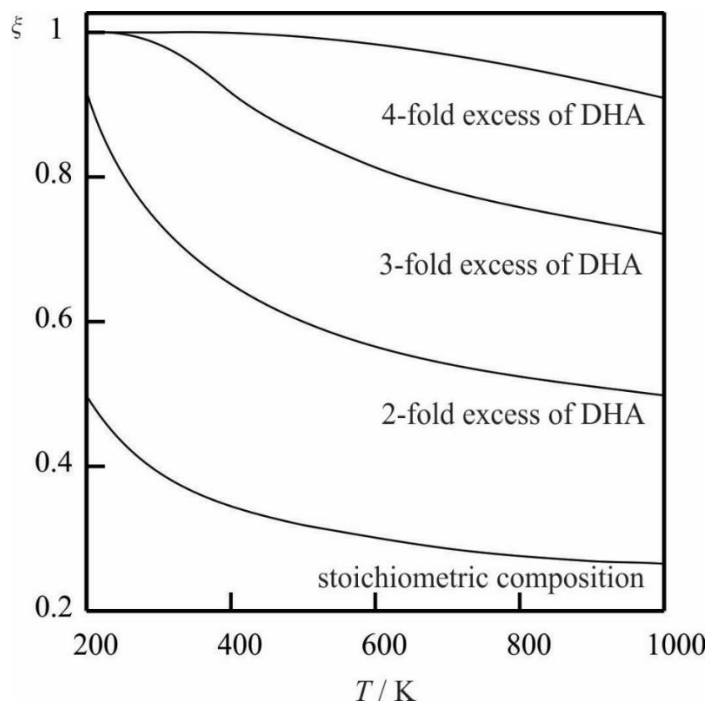
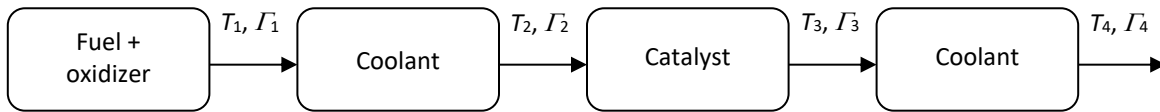


**FIGURE 25.** Dependence of degree of  $C_{60}$  conversion  $\xi$  on temperature and excess of DHA in reaction. Adapted by permission from Springer [52], © 2010.

5.6. Thermodynamics of processes in gas-generating systems [145, 146, 147]

Gas generators using a fuel's combustion energy to decompose a coolant are deployed for creating controlled atmospheres as well as working bodies in pneumatic devices and rocket technology. We carried out a multiphase, multicomponent thermodynamic analysis of the potential increase of gas production in such gas generators due to catalytical ammonia dissociation and water vapor conversion under isothermal-isobaric conditions. Also, we developed a method for estimation of the fuel/coolant ratios in adiabatic conditions for the following coolants:  $\text{NH}_4\text{HCO}_3$ ,  $(\text{NH}_4)_2\text{CO}_3$ ,  $(\text{COO})_2(\text{NH}_4)_2$ , and  $\text{CH}_3\text{OH}$ . Due to kinetic limitations, a catalytic conversion is possible at  $T > 700 \text{ K}$ . Therefore, a stepwise cooling concept was proposed:



Gas production rates  $I_i$  were calculated at different coolant/fuel mass ratios ( $m_1/m_2$ ) (figure 26). The theoretical gas production rate  $I_3$  reached a maximum at a certain  $m_1/m_2$  ratio. Conversion of fuel gases without the coolant increased the gas production rates by 15 %.

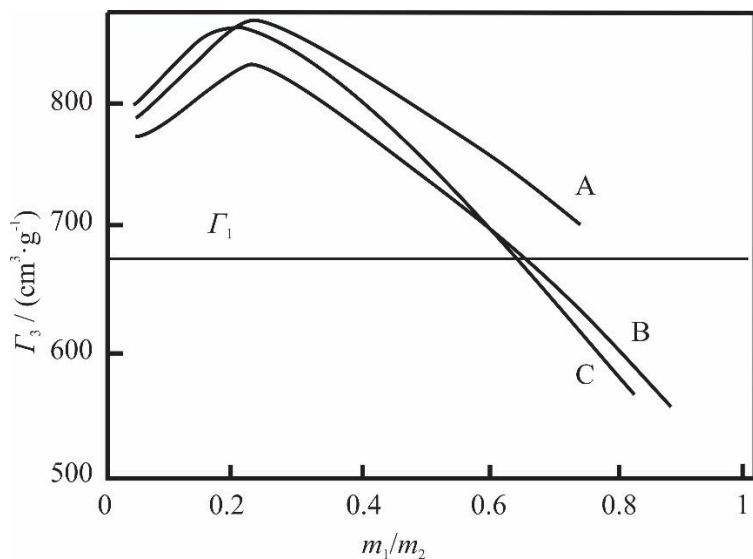


**FIGURE 26.** Plot of the gas-production rate as a function of the coolant/propellant mass ratio for the following coolants: A –  $(\text{NH}_4)_2\text{C}_2\text{O}_4$ ; B –  $\text{NH}_4\text{HCO}_3$ ; and C –  $(\text{NH}_4)_2\text{CO}_3$ . Adapted from [146].

A cooling system for a Venus descent module was developed with participation of Dr. Isaac I. Kantorovich. It was demonstrated that an assembly of concentric spherical jackets, either evacuated or filled with the decomposing coolants, could keep the module temperature below 373 K for at least 24 h.

### 5.7. Vaporization and diffusion of pheromones [148]

Physicochemical parameters of vaporization and diffusion of pheromones were studied to inform design of devices with the optimized use of expensive biologically active substances that act through the gas phase. For two pheromones, 2-methyl-3-buten-2-ol and  $\alpha$ -pinene, diffusion coefficients in the air, permeability of polyethylene films of different thickness for gas-phase pheromones, and entrainment rates from various carriers were determined. A mathematical model was developed for the propagation of the pheromone of *i.typographus* in the atmosphere and the isoconcentration lines were determined. The model considered the wind speeds and distribution in

the Republic of Belarus. Together, these data provided a foundation for how to more effectively deploy pheromones by keeping the required concentration of the pheromone within the optimal limits.

## *5.8. Substantiation of rational ways of biomass conversion into fuel [149, 150, 151, 152]*

### *5.8.1. Thermodynamic properties of macro components of crops [153, 154, 155]*

Energies of combustion and heat capacities were measured for the samples of microcrystalline, wood sulfite, straw, and wood amorphous celluloses, cuproammonium and sulfuric lignins, starch, D-glucose, and levoglucosan. The obtained values of thermodynamic properties of cellulose and lignin were used for analysis of the thermodynamically controlled processes of pyrolysis and thermal gasification over the range  $T = (300 \text{ to } 1700) \text{ K}$  (figures 27, 28, 29, and 30). It was found that hydrothermal gasification of these materials into the  $\text{CO} + \text{H}_2$  mixture led to approximately 15 % loss of the lower energy value compared to direct combustion.

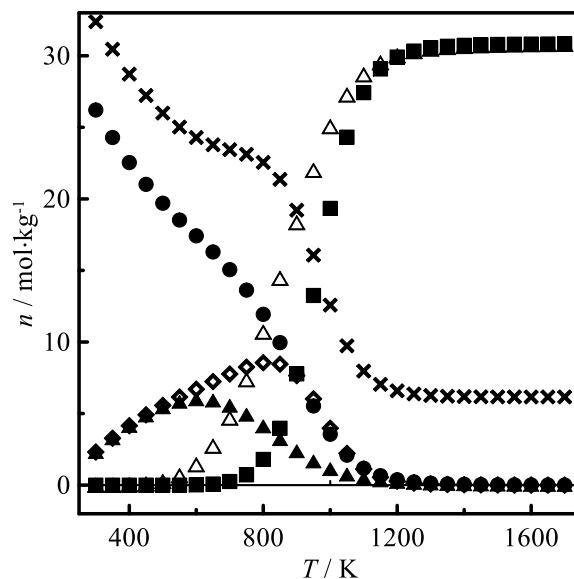


**FIGURE 27.** Equilibrium compositions for cellulose pyrolysis: ●, H<sub>2</sub>O; ◇, CO<sub>2</sub>; ▲, CH<sub>4</sub>; ×, C; ■, CO; △, H<sub>2</sub>.  $P = 0.1$  MPa. Adapted with permission from Ref. [153]. © 2011 American Chemical Society.

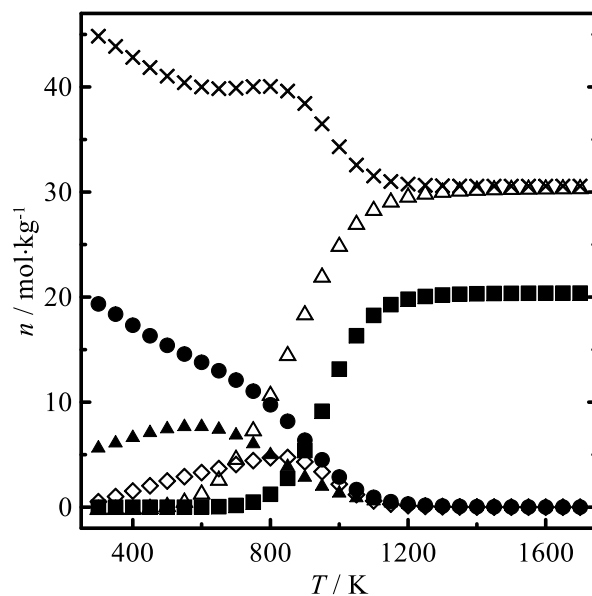


**FIGURE 28.** Equilibrium compositions of pyrolysis for sulfuric lignin at  $P = 0.1$  MPa: ●, H<sub>2</sub>O; ◇, CO<sub>2</sub>; ▲, CH<sub>4</sub>; ×, C; ■, CO; △, H<sub>2</sub>. Adapted with permission from Ref. [154]. © 2012 American Chemical Society.

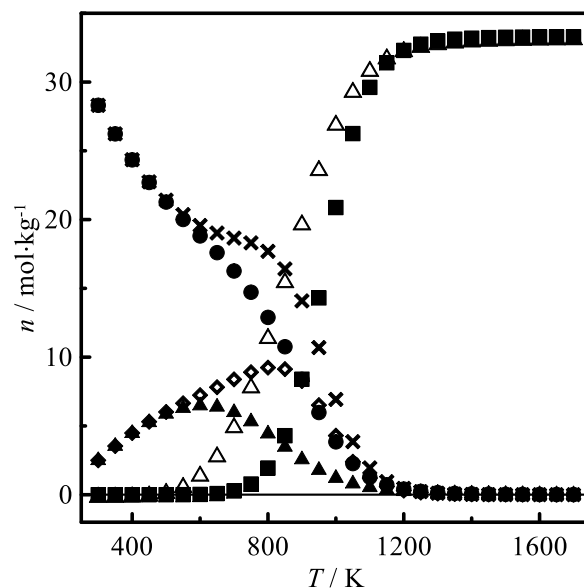


**FIGURE 29.** Equilibrium composition of reaction mixture for the initial composition (cellulose:H<sub>2</sub>O = 1:1): •, H<sub>2</sub>O; ◊, CO<sub>2</sub>; ▲, CH<sub>4</sub>; ×, C; ■, CO; △, H<sub>2</sub>. *P* = 0.1 MPa. Adapted with permission from Ref. [153]. © 2011 American Chemical Society.

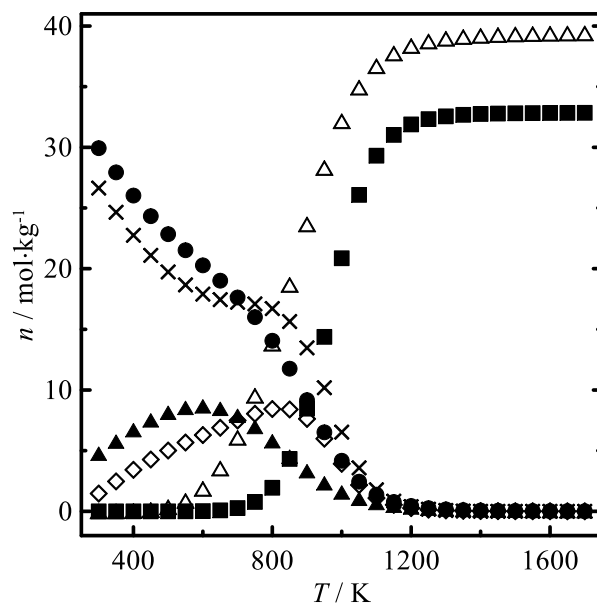


**FIGURE 30.** Equilibrium composition of reaction mixture for the initial composition sulfuric lignin:H<sub>2</sub>O = 1:6 at *P* = 0.1 MPa: •, H<sub>2</sub>O; ◊, CO<sub>2</sub>; ▲, CH<sub>4</sub>; ×, C; ■, CO; △, H<sub>2</sub>. Adapted with permission from Ref. [154]. © 2012 American Chemical Society.

5.8.2. Strategy of plant biomass conversion into fuel [151, 152, 156, 157]

Boyles concluded [158] that strategies for converting biomass of agricultural plants into fuels should be based on an analysis of their composition, combustion energies, processing methods, and economic and social aspects of the products obtained. The energy density of hydrocarbon fuels is higher than the corresponding values for dry plant biomass, but the cost of 1 GJ obtained from the biomass may be lower than that of the hydrocarbon fuels. Energy density is critical for the operation of vehicular energy units. Therefore, in the foreseeable future, preference will be given to the more expensive fuels with a high energy density. Stationary power plants can use renewable energy supplies that are significantly less expensive. Although it is possible to produce energy-rich liquid and gaseous fuels from renewable biomass, it should be borne in mind that energy degradation occurs during its chemical and biochemical processing (Table 6). The lowest degradation of energy occurs when fuels of natural consistency are produced. This primarily applies to solid fuels in the form of pellets or briquettes.

**TABLE 6**

Enthalpy of combustion  $\Delta_c H^\circ$  at  $T = 298.15$  K for fuels, plant raw materials, and energy loss in the production of fuels from plant crops

| Dry fuel     | $\Delta_c H^\circ$ of fuel /<br>MJ·kg <sup>-1</sup> | Raw<br>material | $\Delta_c H^\circ$ of<br>dry raw<br>material<br>/ MJ·kg <sup>-1</sup> | $\Delta_c H^\circ$ for material<br>of natural<br>wetness <sup>1</sup> /<br>MJ·kg <sup>-1</sup> | Mass $m$ of<br>dry material<br>/ kg per 1 kg<br>of fuel | Energy loss<br>factor<br><sup>3</sup> |
|--------------|---|-----------------|---|--|---|---------------------------------------|
| Fuel ethanol | 29.5  | potato          | 16  | 4 (0.75)   | 12  | 1.6                                   |
|              |   | rye             | 16 <sup>2</sup>   | 13.8 (0.14)  | 5   | 2.3                                   |

|              |      |            |                 |             |     |      |
|--------------|------|------------|-----------------|-------------|-----|------|
|              |      | corn seeds | 16 <sup>2</sup> | 13.8 (0.14) | 4   | 1.9  |
|              |      | wood       | 20              | 17 (0.15)   | 7   | 4.0  |
| Rapeseed oil | 39.6 | rape seeds | 29.4            | 25.3 (0.14) | 3.5 | 2.2  |
| Fuel pellets | 18   | straw      | 18              | 15.7 (0.13) | 1.2 | 1.05 |
| and          |      |            |                 |             |     |      |
| briquettes   |      |            |                 |             |     |      |

---

<sup>1</sup> Mass fraction of water is given in the parentheses.

<sup>2</sup> Values estimated from energies of combustion for the samples with natural wetness

<sup>3</sup> Calculated as  $m \cdot \Delta_c H^\circ(\text{material of natural wetness}) / \Delta_c H^\circ(\text{fuel})$ .

The technical and economic analysis of the ways for processing agricultural plant biomass leads to the following economically and socially justified conclusions [152]:

- Food and feed components of agricultural crops should be processed into food and feed, but not fuels.
- Non-food and non-feed parts of biomass (straw, stem residues, threshed cobs, *etc.*) are a valuable raw material to produce good-quality fuels.

The resources of straw, stalk and other non-food and non-feed parts of biomass in the Republic of Belarus can be as large as  $(7.5 \text{ to } 15) \cdot 10^9$  kilograms per year [152]. This, in principle, supports production of solid fuels in the amount of  $(3.2 \text{ to } 6.5) \cdot 10^9$  kilograms of oil equivalent per year, which is (18 to 36) % of the current annual fuel consumption [159] in Belarus.

### 5.8.3. Solid fuels from energy-rich crops

One of the promising directions for the development of renewable energy is the search for and introduction of energy-rich plant crops with a yield of dry biomass above  $10^6$  kg·km<sup>-2</sup> (10 metric tons per hectare) per year. We demonstrated that this approach can be extremely effective for the agricultural economy in some regions of Belarus. Per the cadastral appraisal, the fertility of almost 24 % of arable land in Belarus ( $\sim 11 \cdot 10^3$  km<sup>2</sup>) is below 25 points on a 100-point scale [160]. On these soils, the yield of cereal crops does not exceed  $10^4$  kg·point<sup>-1</sup>·km<sup>-2</sup>, or less than  $(2.0$  to  $2.5) \cdot 10^5$  kg·km<sup>-2</sup>. The use of these lands for agricultural crop production is economically unprofitable.

One of the cost-efficient ways of using low-fertility lands in Belarus could be cultivation of energy-rich plant crops to produce solid fuels. The Central Botanical Garden of the National Academy of Sciences of Belarus has successfully tested the technologies of growing energy-rich crops. These technologies provided a high yield of dry biomass, were undemanding to soil fertility and fertilizers, easy to grow, and could provide a high yield of biomass without replanting for (5 to 30) years and a potential return of the land to agricultural production with an increased fertility. Jerusalem artichoke (*Helianthus tuberosus* L.), cup plant (*Silphium perfoliatum* L.), Weyrich's knotweed (*Aconogonon weyrichii*), and giant miscanthus (*Miscanthus × giganteus*) were found to be the most promising species. We estimated the energy efficiency for these crops using the results obtained in our laboratory (Table 7).

Cultivation of energy-rich crops on low-fertility lands with subsequent processing of dry biomass into fuel pellets is economically efficient [161]. The potential resource of this type of solid fuel in the Republic of Belarus is at least  $(5$  to  $7) \cdot 10^9$  kg per year.

**TABLE 7**

Energy efficiency of stem biomass for energy-rich crops

| Crop                | Yield of dry biomass /<br>10 kg·m <sup>-2</sup> a,b | $\Delta_c H^\circ$ /<br>MJ·kg <sup>-1</sup> c | $\Delta_c H^\circ$ / 10<br>MJ·m <sup>-2</sup> d | Mass of oil<br>equivalent /<br>10 kg·m <sup>-2</sup> a |
|---------------------|---|---|---|--|
| Jerusalem artichoke | 15  | 17.3  | 260   | 6.2  |
| Cup plant           | 14  | 16.5  | 231   | 5.5  |
| Weyrich's knotweed  | 12  | 17.4  | 209   | 5.0  |
| Giant miscanthus    | 16  | 16.0  | 256   | 6.1  |

<sup>a</sup> unit equivalent to 1 metric ton per hectare<sup>b</sup> [162]<sup>c</sup> at  $T = 298.15$  K and  $P = 0.1$  MPa<sup>d</sup> unit equivalent to 1 GJ per hectare

## 6. Notes

The authors declare no competing financial interest.

## Acknowledgments

We appreciate the administrative support provided to us for many years by the former Head of Department of Chemistry Prof. Gennady A. Branitsky and by the late Director of the Institute of Physical and Chemical Research Academician Vadim V. Sviridov. We acknowledge enormous loss we felt with the tragic passing of Prof. Alexander A. Kozyro. It was very hard for us to keep

our research going after that. We also remember with great appreciation contributions of P. A. Poleschuk and E. N. Kozyrsky.

It was enjoyable to work with our many colleagues, and we want to express our appreciations to the late Prof. Kenneth N. Marsh (University of Canterbury, Christchurch, New Zealand), Dr. Joseph W. Magee (National Institute of Standards and Technology, Boulder, USA), Profs. Andreas Heinz and Sergey Verevkin (University of Rostock, Germany), the late Prof. Viktor P. Kolesov (Moscow State University, Russia), Prof. Alexey K. Baev (Belarusian State Technological University, Minsk, Belarus), Drs. E. A. Sorkin (VNIIFTRI, Moscow, Russia), E. A. Miroshnichenko (Institute of Chemical Physics of Russian Academy of Sciences, Moscow, Russia), Prof. Ya. S. Vygodsky (Institute of Organoelement Compounds of Russian Academy of Sciences, Moscow, Russia), Drs. A. S. Shaplov (Luxembourg Institute of Science and Technology, Hautcharage, Luxembourg), S. E. Dem'yanov (SSPA "Scientific – Practical Materials Research Center of Academy of Sciences of Belarus"), and Isaac I. Kantorovich (Intel Corp., Boston, USA). This article is, in part, a contribution of NIST, and is not subject to copyright in the United States. Trade names are provided only to specify procedures adequately and do not imply endorsement by the National Institute of Standards and Technology. Similar products by other manufacturers may be found to work as well or better.

## References

---

1. F. D. Rossini, K. S. Pitzer, R. L. Arnett, R. M. Braun, G. C. Pimentel, Selected Values of Physical and Thermodynamic Properties of Hydrocarbons and Related Compounds, Carnegie Press, Pittsburgh, PA, 1953.
2. Molecular Structure and Statistical Thermodynamics: Selected Papers of Kenneth S. Pitzer, K. S. Pitzer (Ed.), World Scientific, Singapore, 1993.
3. E. F. Westrum, Jr., J. P. McCullough, Physics of Crystals, in: D. Fox, M. M. Labes, A. Weissberger (Eds.), Physics and Chemistry of the Organic Solid State, Interscience, New York, 1963, Vol. 1, pp. 1–178.
4. S. M. Skuratov, V. P. Kolesov, A. F. Vorobyov, Thermochemistry, Vols. 1 and 2, Moscow State University, Moscow, 1964.
5. V. M. Tatevsky, Classical Theory of Molecular Structure and Quantum Mechanics, Khimiya, Moscow, 1973.
6. G. J. Kabo, A. V. Blokhin, A. G. Kabo, Investigation of Thermodynamic Properties of Organic Substances, in: O. A. Ivashkevich (Ed.), Chemical Problems of the Development of New Materials and Technologies, Vol. 1, Belarusian State University, Minsk, 2003, pp. 176–192.
7. G. J. Kabo, G. N. Roganov, M. L. Frenkel, Thermodynamics and Equilibria of Isomers, Universitetskoye, Minsk, 1986.
8. G. J. Kabo, G. N. Roganov, M. L. Frenkel, Thermodynamics and Equilibria of Isomers, in: M. Frenkel (Ed.), Thermochemistry and Equilibria of Organic Compounds, VCH, New York, 1993.
9. V. I. Fedoseenko, I. A. Yursha, G. J. Kabo, Dokl. Akad. Nauk BSSR 27 (1983) 926-929.

- 
10. V. I. Fedoseenko, I. A. Yursha, G. J. Kabo, Dokl. Akad. Nauk BSSR 28 (1984) 1109-1112.
  11. G. J. Kabo, D. N. Andreevsky, Neftekhimiya 3 (1963) 764-770.
  12. M. M. Brazhnikov, G. J. Kabo, D. N. Andreevsky, I. A. Yursha, Izvestiya Vyssh. Ucheb. Zaved., Khim. Khim. Tekhnol. 14 (1971) 510-514.
  13. G. N. Roganov, G. J. Kabo, D. N. Andreevsky, Neftekhimiya 12 (1972) 495-500.
  14. G. N. Roganov, G. J. Kabo, D. N. Andreevsky, K. B. Nikulin, Neftekhimiya 10 (1970) 16-21.
  15. G. J. Kabo, D. N. Andreevsky, Zh. Fiz. Khim. 47 (1973) 272-273.
  16. Z. A. Radyuk, G. J. Kabo, D. N. Andreevsky, Neftekhimiya 13 (1973) 356-360.
  17. I. A. Yursha, G. J. Kabo, Zh. Fiz. Khim. 50 (1976) 558-559.
  18. Z. A. Radyuk, G. J. Kabo, D. N. Andreevsky, Neftekhimiya 12 (1972) 679-686.
  19. G. J. Kabo, D. N. Andreevsky, Z. A. Radyuk, Neftekhimiya 10 (1970) 330-334.
  20. G. J. Kabo, D. N. Andreevsky, G. A. Savinetskaya, Neftekhimiya 7 (1967) 364-368.
  21. I. A. Yursha, G. J. Kabo, Zh. Fiz. Khim. 49 (1975) 1302-1303.
  22. I. A. Yursha, G. J. Kabo, D. N. Andreevsky, 14 (1974) 688-693.
  23. S. V. Petrova-Kuminskaya, G. N. Roganov, G. J. Kabo, Neftekhimiya 23 (1983) 489-494.
  24. S. V. Petrova-Kuminskaya, G. N. Roganov, G. J. Kabo, Neftekhimiya 24 (1984) 485-490.
  25. G. J. Kabo, D. N. Andreevsky, Neftekhimiya 5 (1965) 132-135.
  26. G. N. Roganov, G. J. Kabo, D. N. Andreevsky, Zh. Org. Khim. 5 (1969) 2097-2102.
  27. G. E. Esipenok, G. J. Kabo, D. N. Andreevsky, Zh. Fiz. Khim. 47 (1973) 739.
  28. D. N. Andreevsky, G. J. Kabo, G. E. Esipenok, Zh. Fiz. Khim. 48 (1974) 1614.
  29. G. E. Esipenok, G. J. Kabo, D. N. Andreevsky, Zh. Fiz. Khim. 49 (1975) 3008.
  30. G. J. Kabo, M. L. Frenkel, J. Chem. Thermodyn. 15 (1983) 377-381.

- 
31. M. L. Frenkel, G. J. Kabo, G. N. Roganov, Thermodynamic Characteristics of Isomerization Reactions, Universitetskoye, Minsk, 1988.
32. M. L. Frenkel, G. J. Kabo, G. N. Roganov Thermodynamic Properties of Isomerization Reactions, Hemisphere, New York, 1992.
33. D. H. Zaitsau, Y. U. Paulechka, A. V. Blokhin, A. V. Yermalayeu, A. G. Kabo, M. R. Ivanets, J. Chem. Eng. Data 54 (2009) 3026-3033.
34. A. B. Bazyleva, A. V. Blokhin, A. G. Kabo, G. J. Kabo, V. N. Emel'yanenko, S. P. Verevkin, J. Chem. Thermodyn. 40 (2008) 509-522.
35. F. Pavese, V. M. Malyshev, Adv. Cryog. Eng. 40 (1994) 119-124.
36. A. V. Blokhin, Y. U. Paulechka, G. J. Kabo, J. Chem. Eng. Data 51 (2006) 1377-1388.
37. A. G. Kabo, V. V. Diky, Thermochim. Acta 347 (2000) 79-84.
38. D. Zaitsau, G. J. Kabo, A. A. Kozyro, V. M. Sevruk, Thermochim. Acta 406 (2003) 17-28.
39. D. H. Zaitsau, Y. U. Paulechka, G. J. Kabo, V. M. Sevruk, Influence of the Anisotropy of the Gas Pressure in the Knudsen Cell on the Values of Saturated Vapor Pressures and the Enthalpy of Evaporation, in: O. A. Ivashkevich (Ed.), Chemical Problems of the Development of New Materials and Technologies, Vol. 2, Belarusian State University, Minsk, 2003, pp. 251–263.
40. D. H. Zaitsau, S. P. Verevkin, Y. U. Paulechka, G. J. Kabo, V. M. Sevruk, J. Chem. Eng. Data 48 (2003) 1393-1400.
41. G. J. Kabo, G. N. Roganov, Dokl. Akad. Nauk BSSR 30 (1986) 832-835.
42. O. E. Grikina, V. M. Tatevsky, Vestn. Moskovsk. Univ. Ser. 2, 29 (1988) 22-26.
43. G. N. Roganov, G. J. Kabo, Vestn. Beloruss. Gos. Univ. Ser. 2, (1978) 3-6.
44. G. J. Kabo, A. A. Kozyro, V. V. Diky, V. V. Simirsky, J. Chem. Eng. Data 40 (1995) 371-393.

- 
45. V. V. Simirsky, G. J. Kabo, M. L. Frenkel, *J. Chem. Thermodyn.* 19 (1987) 1121-1127.
46. G. J. Kabo, A. A. Kozyro, V. V. Diky, *J. Chem. Eng. Data* 40 (1995) 160-166.
47. V. N. Emel'yanenko, G. J. Kabo, S. P. Verevkin, *J. Chem. Eng. Data* 51 (2006) 79-87.
48. G. Kabo, E. Paulechka, M. Frenkel, Heat Capacities and Phase Transitions for the Dynamic Chemical Systems: Conformers, Tautomers, Plastic Crystals, and Ionic Liquids, in: E. Wilhelm, T. M. Letcher (Eds.), *Heat Capacities: Liquids, Solutions and Vapours*, RSC, London, 2010, pp. 390-420.
49. J. D. van der Waals, Ph. Kohnstamm, *Lehrbuch der Thermostatik*, Verlag von J. A. Barth, Leipzig, 1927.
50. P. A. Poleschuk, G. J. Kabo, M. L. Frenkel, *Zh. Fiz. Khim.* 62 (1968) 1105-1109.
51. M. L. Frenkel, G. J. Kabo, K. N. Marsh, G. N. Roganov, R. C. Wilhoit, *Thermodynamics of Organic Compounds in the Gas State*, Vols. 1 and 2, TRC, College Station, 1994.
52. G. J. Kabo, L. S. Karpushenkava, Y. U. Paulechka, Thermodynamic Properties of Fullerene Hydrides  $C_{60}H_{2n}$  and Equilibria of Their Reactions, in: F. Cataldo, S. Iglesias-Groth (Eds.), *Carbon Materials: Chemistry and Physics*, Vol. 2, Springer, New York, 2010, pp. 55-83.
53. L. S. Karpushenkava, G. J. Kabo, A. B. Bazyleva, *J. Mol. Struct.: Theochem* 913 (2009) 43-49.
54. G. J. Kabo, A. V. Blokhin, M. B. Charapennikau, A. G. Kabo, V. M. Sevruk, *Thermochim. Acta*, 345 (2000) 125-133.
55. A. B. Bazyleva, A. V. Blokhin, G. J. Kabo, M. B. Charapennikau, V. N. Emel'yanenko, S. P. Verevkin, V. Diky, *J. Phys. Chem. B* 115 (2011) 10064-10072.
56. L. S. Karpushenkava, G. J. Kabo, A. B. Bazyleva, A. V. Blokhin, A. G. Kabo, *Thermochim. Acta*, 459 (2007) 104-110.

- 
57. G. J. Kabo, A. A. Kozyro, A. P. Marchand, V. V. Diky, V. V. Simirsky, L. S. Ivashkevich, A. P. Krasulin, V. M. Sevruk, M. L. Frenkel, *J. Chem. Thermodyn.*, 26 (1994) 129-142.
58. G. J. Kabo, A. A. Kozyro, V. V. Diky, V. V. Simirsky, L. S. Ivashkevich, A. P. Krasulin, V. M. Sevruk, A. P. Marchand, M. L. Frenkel, *J. Chem. Thermodyn.*, 27 (1995) 707-720.
59. V. V. Diky, G. J. Kabo, *Vestn. Beloruss. Gos. Univ. Ser. 2.* (1992) 37.
60. G. J. Kabo, D. N. Andreevsky, S. Ya. Karaseva, *Theor. Eksp. Khim.* 4 (1968) 843-847.
61. V. V. Diky, N. V. Martsinovich, G. J. Kabo, *J. Phys. Chem. A*, 105 (2001) 4969-4973.
62. G. J. Kabo, V. V. Diky, A. A. Kozyro, A. P. Krasulin, V. M. Sevruk, *J. Chem. Thermodyn.* 27 (1995) 953-967.
63. V. V. Diky, G. J. Kabo, A. A. Kozyro, A. P. Krasulin, V. M. Sevruk, *J. Chem. Thermodyn.* 25 (1993) 1169-1181.
64. G. J. Kabo, I. A. Yursha, M. L. Frenkel, P. A. Polechuk, V. I. Fedoseenko, *J. Chem. Thermodyn.* 20 (1988) 429-437.
65. G. J. Kabo, A. A. Kozyro, A. P. Krasulin, V. M. Sevruk, L. S. Ivashkevich, *J. Chem. Thermodyn.* 25 (1993) 485-493.
66. E. N. Stepurko, Y. U. Paulechka, A. V. Blokhin, G. J. Kabo, S. V. Voitekhovich, A. S. Lyakhov, S. V. Kohut, T. E. Kazarovets, *Thermochim. Acta* 592 (2014) 10-17.
67. T. V. Soldatova, G. J. Kabo, A. A. Kozyro, M. L. Frenkel, *Zh. Fiz. Khim.* 64 (1990) 336-343.
68. A. A. Kozyro, G. J. Kabo, T. V. Soldatova, V. V. Simirsky V. I. Gogolinsky, A. P. Krasulin, M. M. Dudarevich, *Zh. Fiz. Khim.* 66 (1992) 2583-2590.
69. Y. U. Paulechka, G. J. Kabo, A. V. Blokhin, O. A. Vydrov, J. W. Magee, M. Frenkel, *J. Chem. Eng. Data* 48 (2003) 457-462.

- 
70. Y. U. Paulechka, G. J. Kabo, V. N. Emel'yanenko, *J. Phys. Chem. B* 112 (2008) 15708-15717.
71. A. B. Bazyleva, G. J. Kabo, Y. U. Paulechka, D. H. Zaitsau, A. V. Blokhin, *Thermochim. Acta* 436 (2005) 56-67.
72. G. J. Kabo, A. V. Blokhin, A. A. Kozyro, V. V. Diky, *Thermochim. Acta* 290 (1997) 13-30.
73. A. A. Kozyro, G. J. Kabo, A. P. Krasulin, V. M. Sevruk, V. V. Simirsky, M. S. Sheiman, M. Frenkel, *J. Chem. Thermodyn.* 25 (1993) 1409-1417.
74. E. A. DiMarzio, F. Dowell, *J. Appl. Phys.*, 1979, 50, 6061-6066.
75. A. V. Blokhin, *Energy States of Molecules in Plastic Crystals of Organic Substances*, in: O. A. Ivashkevich (Ed.), *Chemical Problems of the Development of New Materials and Technologies*, Vol. 2, Belarusian State University, Minsk, 2003, pp. 200–229.
76. A. V. Blokhin, M. B. Charapennikau, G. J. Kabo, *Energy States of Molecules in Plastic Crystals of Cage Hydrocarbons and their Hydroxy Derivatives*, in: V. V. Sviridov (Ed.), *Selected Publications*, Vol. 5, Belarusian State University, Minsk, 2001, pp. 429-445.
77. G. J. Kabo, A. A. Kozyro, M. Frenkel, A. V. Blokhin, *Mol. Cryst. Liq. Cryst.* 326 (1999) 333-355.
78. A. B. Bazyleva, A. V. Blokhin, G. J. Kabo, A. G. Kabo, Y. U. Paulechka, *J. Chem. Thermodyn.* 37 (2005) 643-657.
79. G. J. Kabo, A. V. Blokhin, A. A. Kozyro, V. V. Diky, L. S. Ivashkevich, A. P. Krasulin, V. M. Sevruk, M. Frenkel, *Thermochim. Acta* 313 (1998) 111-124.
80. M. B. Charapennikau, A. V. Blokhin, G. J. Kabo, A. G. Kabo, V. V. Diky, A. G. Gusakov, *Thermochim. Acta*, 382 (2002) 109-118.

- 
81. M. B. Charapennikau, A. V. Blokhin, G. J. Kabo, V. M. Sevruk, A. P. Krasulin, *Thermochim. Acta* 405 (2003) 85-91.
82. M. B. Charapennikau, A. V. Blokhin, G. J. Kabo, A. G. Kabo, A. G. Gusakov, *Vesti Nats. Akad. Nauk Belarusi, Ser. Khim.*, Issue 2 (2001) 43-46.
83. M. B. Charapennikau, G. J. Kabo, A. V. Blokhin, A. G. Gusakov, *Russ. J. Phys. Chem.* 77 (2003) 368-373.
84. M. B. Charapennikau, A. V. Blokhin, A. G. Kabo, G. J. Kabo, *J. Chem. Thermodyn.* 35 (2003) 145-157.
85. A. B. Bazyleva, A. V. Blokhin, G. J. Kabo, A. G. Kabo, V. M. Sevruk, *Thermochim. Acta* 451 (2006) 65-72.
86. A. B. Bazyleva, G. J. Kabo, A. V. Blokhin, *Physica B: Condensed Matter.* 383 (2006) 243-252.
87. A. Kazakov, J. W. Magee, R. D. Chirico, E. Paulechka, V. Diky, C. D. Muzny, K. Kroenlein, M. Frenkel, *NIST Standard Reference Database 147: NIST Ionic Liquids Database - (ILThermo)*, Version 2.0, National Institute of Standards and Technology, Gaithersburg MD, 20899, <http://ilthermo.boulder.nist.gov>. (Retrieved September 11, 2018).
88. J. Magee, G. Kabo, M. Frenkel, *Physical Property Measurements and Comprehensive Data Retrieval System for Ionic Liquids*, in: R. D. Rogers, K. R. Seddon (Eds.), *ACS Symposium Series, Ionic Liquids III: Fundamentals, Progress, Challenges and Opportunities*, Amer. Chem. Soc., Washington DC, 2004, pp. 160–174.
89. Y. U. Paulechka, *J. Phys. Chem. Ref. Data* 39 (2010) 033108.
90. E. Paulechka, C. Muzny. *Ionic liquids*, in: J. R. Rumble (Ed.), *CRC Handbook on Chemistry and Physics*, 98<sup>th</sup> Ed., 2017.

- 
91. Y. U. Paulechka, D. H. Zaitsau, G. J. Kabo, A. A. Strechan. *Thermochim. Acta* 439 (2005) 158-160.
92. D. H. Zaitsau, G. J. Kabo, A. A. Strechan, Y. U. Paulechka, A. Tschersich, S. P. Verevkin, A. Heintz, *J. Phys. Chem. A* 110 (2006) 7303-7306.
93. Y. U. Paulechka, G. J. Kabo, A. V. Blokhin, A. S. Shaplov, E. I. Lozinskaya, D. G. Golovanov, K. A Lyssenko, A. A. Korlyukov, Ya. S Vygodskii, *J. Phys. Chem. B* 113 (2009) 9538-9546.
94. Y. U. Paulechka, G. J. Kabo, A. V. Blokhin, A. S. Shaplov, E. I. Lozinskaya, Ya. S. Vygodskii, *J. Chem. Thermodyn.* 39 (2007) 158-166.
95. Y. U. Paulechka, A. V. Blokhin, G. J. Kabo, *Thermochim. Acta* 604 (2015) 122-128.
96. Y. U. Paulechka, A. G. Kabo, A. V. Blokhin, G. J. Kabo, M. P. Shevelyova, *J. Chem. Eng. Data* 55 (2010) 2719-2724.
97. Y. U. Paulechka, A. V. Blokhin, G. J. Kabo, A. A. Strechan, *J. Chem. Thermodyn.* 39 (2007) 866-877.
98. Y. U. Paulechka, A. V. Blokhin. *J. Chem. Thermodyn.* 79 (2014) 94-99.
99. A. A. Strechan, Y. U. Paulechka, A. V. Blokhin, G. J. Kabo, *J. Chem. Thermodyn.* 40 (2008) 632-639.
100. A. A. Strechan, A. G. Kabo, Y. U. Paulechka, A. V. Blokhin, G. J. Kabo, A. S. Shaplov, E. I. Lozinskaya, *Thermochim. Acta* 474 (2008) 25-31.
101. G. J. Kabo, A. V. Blokhin, Y. U. Paulechka, A. G. Kabo, M. P. Shymanovich, J. W. Magee, *J. Chem. Eng. Data* 49 (2004) 453-461.
102. E. Paulechka, T. Liavitskaya, A. V Blokhin, *J. Chem. Thermodyn.* 102 (2016) 211-218.

- 
103. A. A. Strechan, Y. U. Paulechka, A. G. Kabo, A. V. Blokhin, G. J. Kabo, *J. Chem. Eng. Data* 52 (2007) 1791-1799.
104. Y. U. Paulechka, S. V. Kohut, A. V. Blokhin, G. J. Kabo, *Thermochim. Acta* 511 (2010) 119-123.
105. A. V. Blokhin, Y. U. Paulechka, A. A. Strechan, G. J. Kabo, *J. Phys. Chem. B* 112 (2008) 4357-4364.
106. E. Paulechka, A. V. Blokhin, A. S. M. C. Rodrigues, M. A. A. Rocha, L. M. N. B. F. Santos, *J. Chem. Thermodyn.* 97 (2016) 331-340.
107. Y. U. Paulechka, G. J. Kabo, *Russ. J. Phys. Chem. A* 82 (2008) 1412-1414.
108. Y. U. Paulechka, *Thermodynamics of Imidazolium-based Ionic Liquids*, D.Sci. Thesis (Phys. Chem.), Belarusian State University, Minsk, 2013.
109. Y. U. Paulechka, *Experimental Investigation and Prediction of Physicochemical Properties for Room-Temperature Ionic Liquids*, in: O. A. Ivashkevich (Ed.), *Chemical Problems of the Development of New Materials and Technologies*, Vol. 3, Belarusian State University, Minsk, 2008, pp. 447–466.
110. Y. U. Paulechka, A. G. Kabo, A. V. Blokhin, G. J. Kabo. *Thermochemical Similarity of 1-Alkyl-3-Methylimidazolium Ionic Liquids and Salts of Alkaline Metals*, in: O. A. Ivashkevich (Ed.), *Sviridov Readings*, Issue 6, Belarusian State University, Minsk, 2010, pp. 184-188.
111. G. J. Kabo, Y. U. Paulechka, D. H. Zaitsau, A. S. Firaha, *Thermochim. Acta* 609 (2015) 7-19.
112. V. V. Diky, G. J. Kabo, *Russ. Chem. Rev.* 69 (2000) 95-104.
113. V. V. Diky, L. S. Zhura, A. G. Kabo, V. Y. Markov, G. J. Kabo, *Fullerene Sci. Tech.* 9 (2001) 543-551.

- 
114. G. J. Kabo, Y. U. Paulechka, A. V. Blokhin, O. V. Voitkevich, T. N. Liavitskaya, A. G. Kabo, *J. Chem. Eng. Data*, 61 (2016) 3849-3857.
115. M. P. Shevelyova, Y. U. Paulechka, G. J. Kabo, A. V. Blokhin, A. G. Kabo, T. M. Gubarevich, *J. Phys. Chem. C* 117 (2013) 4782-4790.
116. J. Y. Howe, C. J. Rawn, L. E. Jones, H. Ow, *Powder Diffraction* 18 (2003) 150-154.
117. L. N. Sidorov, M. A. Yurovskaya, A. Y. Borschevskiy, I. V. Trushkov, I. N. Ioffe, *Fullerenes, Ekzamen, Moscow*, 2005.
118. W. Krätschmer, L. D. Lamb, K. Fostiropoulos, D. R. Huffman, *Nature* 347 (1990) 354-358.
119. J. D. Cox, D. D. Wagman, V. A. Medvedev, *CODATA Key Values for Thermodynamics*, Hemisphere Pub. Corp.: New York, 1989.
120. M. W. J. Chase, *NIST-JANAF Thermochemical Tables, 4th Edition*. *J. Phys. Chem. Ref. Data*, Monograph 9 (1998) 1-1951.
121. G. J. Kabo, O. V. Govin, A. A. Kozyro, *Dokl. Nats. Akad. Nauk Belarusi* 40(6) (1996) 67-71.
122. G. J. Kabo, O. V. Govin, A. A. Kozyro, *Energy* 23 (1998) 383-391.
123. O. V. Govin, G. J. Kabo, *Zh. Fiz. Khim.* 72 (1998) 1964-1966.
124. O. V. Govin, V. V. Diky, G. J. Kabo, A. V. Blokhin, *J. Therm. Anal. Calorim.* 62 (2000) 123-133.
125. M. L. Frenkel, I. A. Yursha, G. J. Kabo, V. I. Fedoseenko, *Zh. Prikl. Khim.* 62 (1989) 1173-1176.
126. A. A. Kozyro, L. I. Marachuk, A. P. Krasulin, I. A. Yursha, G. J. Kabo, *Zh. Prikl. Khim.* 62 (1989) 595-599.

- 
127. M. L. Frenkel, I. A. Yursha, I. I. Kantorovich, Le Tung An, G. J. Kabo, E. M. Golovako, *Khim. Prom.* (1988) 707-710.
128. V. S. Krouk, Z. A. Antonova, G. J. Kabo, I. A. Yursha, V. V. Simirsky, *Khim. Prom.* (1999) 578-582.
129. I. A. Yursha, Z. A. Antonova, V. V. Simirsky, G. J. Kabo, A. A. Kozyro, V. S. Krouk, *Khim. Prom.* (1997) 726-733.
130. A. A. Kozyro, G. J. Kabo, V. S. Krouk, M. S. Sheiman, I. A. Yursha, V. V. Simirsky, A. P. Krasulin, V. M. Sevruk, V. I. Gogolinsky, *J. Chem. Thermodyn.* 24 (1992) 883-895.
131. G. J. Kabo, A. A. Kozyro, V. S. Krouk, V. M. Sevruk, I. A. Yursha, V. V. Simirsky, V. I. Gogolinsky, *J. Chem. Thermodyn.* 24 (1992) 1-13.
132. L. I. Marachuk, A. A. Kozyro, V. V. Simirsky, G. J. Kabo, I. A. Yursha, A. P. Krasulin, V. M. Sevruk, *Zh. Prikl. Khim.* 65 (1992) 875-880.
133. M. P. Shevelyova, G. J. Kabo, A. V. Blokhin, A. G. Kabo, J. A. Yursha, A. A. Rajko, *J. Chem. Eng. Data* 51 (2006) 40-45.
134. V. V. Simirsky, A. A. Kozyro, G. J. Kabo, I. A. Yursha, L. I. Marachuk, *Zh. Prikl. Khim.* 65 (1992) 1638-1645.
135. M. P. Shevelyova, D. H. Zaitsau, Y. U. Paulechka, A. V. Blokhin, G. J. Kabo, S. P. Verevkin, A. Heintz, *J. Chem. Eng. Data* 52 (2007) 1360-1365.
136. M. P. Shevelyova, Y. U. Paulechka, G. J. Kabo, A. S. Halauko, *J. Chem. Eng. Data* 56 (2011) 185-189.
137. M. L. Frenkel, E. A. Gusev, G. J. Kabo, *Zh. Prikl. Khim.* 17 (1983) 212-214.

- 
138. A. A. Kozyro, Thermodynamic Properties of Products of Industrial Synthesis of Urea, Caprolactam, Dimethyl Terephthalate, and Related Compounds, Dr. Sci. Thesis (Phys. Chem.), Belarusian State University, Minsk, 1997.
139. Y. U. Paulechka, A. G. Kabo, A. V. Blokhin, J. Phys. Chem. B 113 (2009) 14742-14746.
140. Y. U. Paulechka, G. J. Kabo, A. V. Blokhin, Dz. S. Firaha, J. Chem. Eng. Data 56 (2011) 4891-4899.
141. G. J. Kabo, Y. U. Paulechka, A. G. Kabo, A. V. Blokhin, J. Chem. Thermodyn. 42 (2010) 1292-1297.
142. L. S. Karpushenkava, Thermodynamic Properties of Cage Hydrocarbons and Hydrofullerenes, Ph.D. Thesis (Phys. Chem.), Belarusian State University, Minsk, 2007.
143. L. S. Karpushenkava, G. J. Kabo, V. V. Diky, Fullerenes, Nanotubes, and Carbon Nanostructures, 15 (2007) 227-247.
144. G. J. Kabo, L. S. Karpushenkava, Y. U. Paulechka. Thermodynamic Properties of Fullerene Hydrides  $C_{60}H_{2n}$  and Equilibria of Their Reactions, in: F. Cataldo, S. Iglesias-Groth (Eds.), Carbon Materials: Chemistry and Physics. Vol. 2. Fullerenes. The Hydrogenated Fullerenes. Springer, 2010, pp. 55-83.
145. M. L. Frenkel, G. J. Kabo, I. I. Kantorovich, E. A. Gusev, A. A. Vecher, V. A. Shandakov, Dokl. Akad. Nauk BSSR 29 (1985) 434-437.
146. G. J. Kabo, M. L. Frenkel, E. A. Gusev, M. A. Kazantseva, I. I. Kantorovich, Teor. Osnovy Khim. Tekhnol. 19 (1985) 533-537.
147. M. A. Kazantseva, M. L. Frenkel, G. J. Kabo, E. A. Gusev, A. A. Vecher, Zh. Prikl. Khim. 18 (1984) 2444-2447.

- 
148. Dz. H. Zaitsau, Y. V. Baranov, G. J. Kabo, Vesti Nats. Akad. Nauk Belarusi, Ser. Khim., Issue 3 (2007) 28-32.
149. G. J. Kabo, A. V. Blokhin, V. V. Simirsky, O. A. Ivashkevich, Application of Biomasses for a Production of Various Types of Fuels, in: O. A. Ivashkevich (Ed.), Chemical Problems of the Development of New Materials and Technologies, Vol. 3, Belarusian State University, Minsk, 2008, pp. 165-179.
150. O. A. Ivashkevich, G. J. Kabo, A. V. Blokhin, V. V. Simirsky, Y. N. Lugovik, Vest. Beloruss. Gos. Univ., Ser. 2 (2009) 4-13.
151. O. A. Ivashkevich, G. J. Kabo, A. V. Blokhin, V. V. Domasevich, V. V. Simirsky, M. P. Shevelyova, Dokl. Nats. Akad. Nauk Belarusi 51(6) (2007) 48-50.
152. G. J. Kabo, A. V. Blokhin, Biomass of Agricultural Crops in Belarus - Food or Fuel?, 2012. [https://agrobeltarus.by/articles/nauka/biomassa\\_selskokhozyaystvennykh\\_kultur\\_belarusi\\_provostvie\\_ili\\_toplivo/](https://agrobeltarus.by/articles/nauka/biomassa_selskokhozyaystvennykh_kultur_belarusi_provostvie_ili_toplivo/) (accessed September 12, 2018).
153. A. V. Blokhin, O. V. Voitkevich, G. J. Kabo, Y. U. Paulechka, M. V. Shishonok, A. G. Kabo, V. V. Simirsky, J. Chem. Eng. Data 56 (2011) 3523-3531.
154. O. V. Voitkevich, G. J. Kabo, A. V. Blokhin, Y. U. Paulechka, M. V. Shishonok, J. Chem. Eng. Data 57 (2012) 1903-1909.
155. G. J. Kabo, O. V. Voitkevich, A. V. Blokhin, S. V. Kohut, E. N. Stepurko, Y. U. Paulechka, J. Chem. Thermodyn. 59 (2013) 87-93.
156. G. J. Kabo, A. V. Blokhin, V. V. Simirsky, O. A. Ivashkevich, Application of Biomasses for a Production of Various Types of Fuels, in: O. A. Ivashkevich (Ed.), Chemical Problems of the Development of New Materials and Technologies, Vol. 3, Belarusian State University, Minsk, 2008, pp. 165-179.

- 
157. O. A. Ivashkevich, G. J. Kabo, A. V. Blokhin, V. V. Simirsky, Y. N. Lugovik, Vest. Beloruss. Gos. Univ., Ser. 2, Issue 1 (2009) 4-13.
158. D. T. Boyles. Bio-energy: Technology, Thermodynamics, and Costs, E. Horwood, New York, 1984.
159. Energy balance of the Republic of Belarus, 2017. [http://www.belstat.gov.by/ofitsialnaya-statistika/publications/izdania/public\\_compilation/index\\_7863/](http://www.belstat.gov.by/ofitsialnaya-statistika/publications/izdania/public_compilation/index_7863/) (accessed September 12, 2018).
160. <http://www.gki.gov.by/uploads/files/Rezultaty-na-1-janvarja-2015-g.pdf> (accessed September 12, 2018).
161. G. J. Kabo, A. V. Blokhin, Justification of the strategy for the reasonable use of biomass of agricultural crops of the Republic of Belarus in the production of fuels, in: Alternative sources of raw materials and fuels, Vol. 1, Belaruskaya Navuka, Minsk, 2014, pp. 48-55.
162. M. I. Yaroshevich, V. I. Podobedov, T. V. Gil', in: Fourth Scientific and Technical Conference Alternative Sources of Raw Material and Fuel, Minsk, May 28–30, 2013. Book of Abstracts, Belaruskaya Navuka, Minsk, 2013, p. 40.